EVALUATION OF RENAL FUNCTION USING FIRST PASS CONTRAST ENHANCED MRI

by

Okan Saldoğan

B.S., in Mechanical Engineering, Yıldız Technical University, 1998

Submitted to the Institute of Biomedical Engineering
in partial fulfillment of the requirements
for the degree of
Master of Science
in
Biomedical Engineering

Boğaziçi University
August, 2005

EVALUATION OF RENAL FUNCTION USING FIRST PASS CONTRAST ENHANCED MRI

APPROVED BY:

Assoc. Prof. Dr. Cengizhan ÖZTÜRK .....
(Thesis Supervisor)

Prof. Dr. Atadan TUNACI .....

Assoc. Prof. Dr. Ahmet ADEMOĞLU .....

DATE OF APPROVAL: 29.August.2005

ACKNOWLEDGMENTS

I would like to thank my thesis supervisor, Assoc. Prof. Dr. Cengizhan ÖZTÜRK for his support and motivation during my thesis study. Without his academic support, experience, deep knowledge and his tolerance this study would not be completed.

I would like to thank Assoc. Prof. Dr. Numan Cem BALCI and Assistant Prof. Dr. Hasan Tahsin SARISOY for their significant contributions to this thesis.

I would like to thank Research Assistants Bora BÜYÜKSARAÇ and Alper YAMAN who listened, helped me and shared their invaluable time.

And to those who directly and indirectly helped me, thank you.

ABSTRACT

EVALUATION OF RENAL FUNCTION USING FIRST PASS CONTRAST ENHANCED MRI

Magnetic Resonance Imaging (MRI) of the kidney has a great potential because the functional parameters, which can be investigated obtained noninvasively are multiple: glomerular filtration, tubular concentration and transit, blood volume and perfusion, diffusion and oxygenation. These require either endogeneous contrast agents, such as water protons (for perfusion and diffusion) or deoxyhemogobin (for oxgenation), or exogeneous contrast agents, such as gadolinium chelates (for filtration and perfusion) or iron oxide particles (for perfusion). In this thesis work, an integrated renal perfusion analysis method is presented, which allows multi-slice animation of renal perfusion images, automatic image registration, quantification of time-intensity curves from desired region of interests (ROI's), and estimation of indexes such as slope, time-to-peak, and contrast enhancement ratio (CER). It was designed as a MATLAB package for reading, displaying, saving and analyzing renal perfusion Magnetic Resonance (MR) images which are in DICOM (Digital Imaging and Communications in Medicine) format. Performance of this package was tested on data obtained from MRI scans on ten volunteers with normal kidney function and both efficient qualitative assessment of differential enhancement of the two kidneys and more accurate time-intensity curve evaluation free from respiratory motion were obtained.

Keywords: MRI, contrast enhanced MRI, renal function, renal perfusion analysis, signal intensity-time curves.

ÖZET

BÖBREK PERFÜZYONUNUN İLK GEÇİŞ MANYETİK REZONANS GÖRÜNTÜLEME İLE DEĞERLENDİRİLMESİ

Böbreğin Manyetik Rezonans Görüntüleme (MRG) teknikleri ile fonksiyonel görüntülenmesi, naninvazif olarak elde edilebilen fonksiyonel parametrelerin çeşitliliği sebebiyle büyük bir potansiyele sahiptir. Bu parametreler, glomerüler filtrasyon, tübüler konsantrasyon ve geçiş, kan hacmi ve perfüzyon, difüzyon ve oksijenlenmedir. Bu teknikler ya su protonları (perfüzyon) veya deoksihemogobin (oksijenlenme) gibi içsel kontrast maddeleri ya da gadalinyum şelatı (filtrasyon ve perfüzyon) veya demir oksit parçacıkları (perfüzyon) gibi dış kaynaklı kontrast maddeleri gerektirirler. Bu tez çalışmasında, manyetik rezonans ile böbreğin fonksiyonel görüntülenmesi incelenmiş ve dinamik böbrek perfüzyon görüntülerinin okunabildiği, gösterilebildiği ve otomatik imge çakıştırması yapılarak istenilen ilgi bölgesinin sinyal yoğunluk-zaman eğrileri üzerinden eğim, tepe noktası ve kontrast artış oranı gibi değerlerinin belirlenebildiği bütünleştirilmiş bir böbrek perfüzyon analiz metodu sunulmaktadır. Formatı DICOM olan böbrek perfüzyon Manyetik Rezonas (MR) görüntülerini okumak, göstermek, kaydetmek ve analiz etmek için bir MATLAB paketi tasarlanmıştır. Bu paket normal böbrek fonksiyonuna sahip on gönüllüden elde edilen MRG taramalarından elde edilen verilerle test edilmiş ve hem iki böbreğin farklılığının kalitatif olarak değerlendirilebilmesi hem de nefes alıp vermeden etkilenmeksizin daha doğru zaman-yoğunluk eğrilerinin değerlendirilebilmesi mümkün olmuştur.

Anahtar Sözcükler: MRG, böbrek işlevi, böbrek perfüzyon analizi, sinyal yoğunluk-zaman eğrileri

TABLE OF CONTENTS

LIST OF FIGURES

LIST OF TABLES

LIST OF SYMBOLS

m	Slope
S_{peak}	Peak Signal
$S_{arrival}$	Arrival Signal
$S_{baseline}$	Baseline Signal
t_{peak}	Peak Time
$t_{arrival}$	Arrival Time

LIST OF ABBREVIATIONS

ACR	American College of Radiology
ADC	Apparent Diffusion Coefficient
BOLD	Blood-Oxygenation Level Dependent
CER	Contrast Enhancement Ratio
DICOM	Digital Imaging and Communications In Medicine
ECF	Extracellular Fluid
FFE	Fast Field Echo
Gd-DTPA	Gadolinium-Diethylene Triamine Pentaacetic Acid
MR	Magnetic Resonance
MRI	Magnetic Resonance Imaging
ROI	Regions of Interest
SNR	Signal to Noise Ratio
TE	Echo Time
TR	Repetition Time

1. INTRODUCTION

1.1 Background and Motivation

Renal function can be affected by a broad range of diseases. Methods to assess renal function have been proven to be useful in the diagnosis and management of these disorders. For example, functional imaging modalities have been used in the assessment of renal artery stenosis [1], in the evolution of renal masses [2], and in the early detection of renal transplant rejection [3].

Dynamic Magnetic Resonance Imaging (MRI) has been in use for some time to retrieve functional information of organs in the human body. In the case of the kidney, dynamic MR imaging is attractive because of its high temporal and spatial resolution, providing the possibility to separate the functional behavior of cortex and medulla. Dynamic contrast-enhanced MRI provides superior anatomic and functional information when compared with ultrasound and diuretic renal scintigraphy. Functional imaging of the kidneys with fast MRI techniques is becoming more prevalent both for clinical and basic science studies. The use of fast imaging techniques has been shown to be useful and very promising for the evaluation of perfusion, diffusion, and oxygenation of the kidneys, in both healthy and disease conditions [4, 5, 6].

1.2 Objectives

The main objective in the proposed thesis work is to develop an analysis module for renal perfusion images. With this module, all the steps necessary for generating quantitative measurements of contrast media uptake and washout for renal perfusion were integrated. This allows for both efficient qualitative assessment of differential enhancement of the two kidneys and more accurate time-intensity curve quantification free from respiratory motion.

1.3 Outline of the Thesis

In the following chapter, the general physiology of the Kidney is presented and Diagnostic techniques for the Kidney are explained briefly. In Chapter 3, MR Renograms are introduced. Renal Perfusion Analysis and its steps in Chapter 4 and the features of our program are presented in Chapter 5. The analysis results of ten volunteers are showed in Chapter 6. The last Chapter is a summary of the basic conclusions and recommendations for future work.

2. THE KIDNEY

2.1 Introduction

The kidneys in a normal adult measure 11 to 14 cm in length from pole to pole and are located retroperitoneally in the lumbar region and form as highly vascular organs an integral part of the systemic circulation. They are concerned with the regulation of the volume and composition of the extracellular fluid and with the elimination of waste products. Each kidney is composed of about one million very tiny tubular structures called "nephrons" (Figure 2.1).

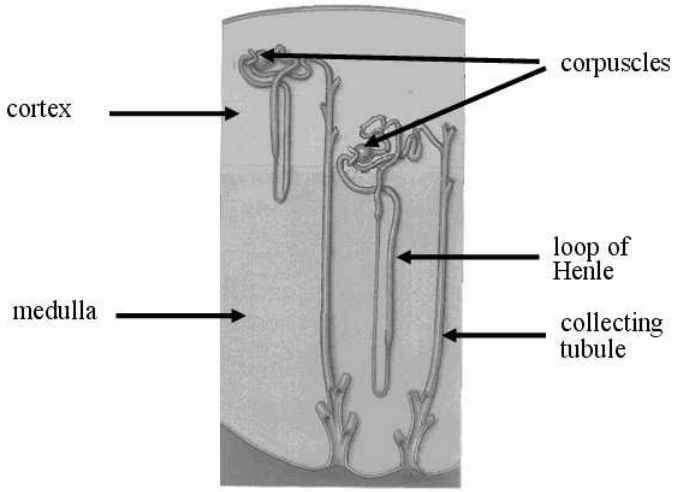

Figure 2.1 Nephrons

The most proximal part of such a nephron is the glomerulus in which the vascular system is closely related to the tubuli and where the blood is filtered. The tubule part of the nephron follows a typical path. Its most proximal part is very tortuous, then the tubule straightens and takes a direct course toward the centre of the kidney, there it makes a hairpin turn and returns in a straight line back to the outer part of the kidney. At that level many nephrons join in straight collecting tubules transporting the urine to the renal hilum and pelvis. The glomeruli are predominantly located in the outer 8 mm of the kidney called the cortex of the kidney and the tubuli are concentrated within the pyramids (Figure 2.2) also called the medulla of the kidney [7, 5].

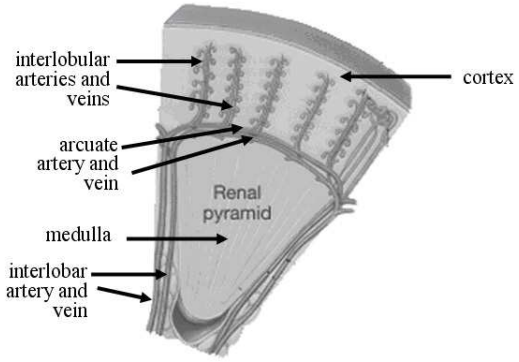

Figure 2.2 Features in a Renal Pyramid

Kidneys are composed of several fused segments or lobes, each having two compartments, i.e., the cortex and the medulla. Cortex and medulla together are called the renal parenchyma (Figure 2.3). The cortex contains glomeruli, proximal and distal convoluted tubules, and a cortical portion of collecting ducts. In the proximal convoluted tubules, approximately two-thirds of water and sodium reabsorption occurs. The medulla contains the loops of Henle and the medullary portion of collecting ducts. The loop of Henle is divided into thin descending, thin ascending, and thick ascending limbs. The medulla can be separated into the outer and the inner medulla. The thick ascending limbs of the loops of Henle, where an active reabsorption of sodium occurs, are within the outer medulla. The medulla is characterized by a corticopapillary osmotic gradient with a progressive increase in urine concentration through the Henle loop [7, 5].

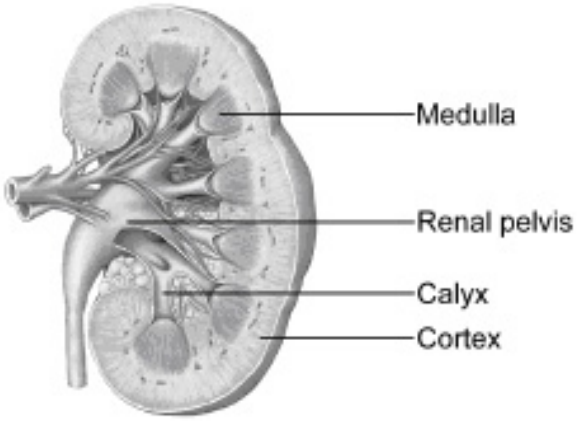

Figure 2.3 Cross section of the kidney

2.2 Diagnostic Techniques for the Kidney

A large variety of diseases can affect the different anatomic elements of the kidney. Many diagnostic techniques are available to detect abnormalities in renal morphology or renal function. Each technique has its own limitations and possibilities.

Urine and blood sample tests give only an impression about the function of both kidneys together. Imaging tests, on the other hand, give morphologic information about each kidney separately and allow for the detection of renal stones, mass lesions or obstructions of the urinary tract. For these roentgenograms, computed tomography or ultrasound examinations are the diagnostic tests of first choice. However the so called medical nephropathies which are diseases of the glomeruli, tubules and interstitial tissue of the renal parenchyma, thus diseases on a microscopic level only without affecting the gross anatomy of the kidney, can not be detected with imaging techniques and often need a radionuclide scan or even a renal biopsy to make a definite diagnosis.

Radionuclide studies provide predominantly functional data and their ability to visualise functional renal tissue, which can not be imaged radiographically, is an advantage of this method. Its inability to show precise anatomical detail is, however, an important drawback. With this technique the flow of a radionuclide tracer through the renal parenchyma can be followed over time with a high temporal but a limited spatial resolution. This method is particularly useful in the post renal transplant management because it can deliver information about renal perfusion, renal filtration and renal excretion. Radionuclide techniques cannot locate functional abnormalities inside the renal parenchyma and cortical and medullary function cannot be differentiated accurately.

Doppler ultrasound can only measure renal blood flow. Furthermore, in a certain percentage of patients the examinations are inadequate because of obesity or the presence of bowel gas. Duplex ultrasound imaging (a combination of pulsed Doppler and B-mode ultrasound) allows the assessment of renal artery stenosis based on flow velocities and morphological appearance [8].

MRI and Computed Tomography (CT) make it possible to obtain images with high temporal and spatial resolution. However, Computed tomography (CT) requires the use of large amounts of iodinated contrast agents. Gadolinium-enhanced MRI more accurately assesses the concentrating ability of the kidneys then does dynamic iodine-enhanced computed tomography (CT), because MRI has a greater sensitivity to gadolinium than does CT to iodine contrast [9].

MRI has the attractive potential for functional kidney imaging by a technique that parallels the radionuclide study principle but may compare favourably in performance. The potential advantages of MRI for evaluating renal tract anomalies offer excellent anatomic resolution and soft tissue contrast, and it does not use ionizing radiation [10].

2.3 Functional MRI of the kidney

Although nuclear medicine is currently the reference method for quantification of most renal functional parameters, MR can compete in many fields. A clear advantage of MRI is its ability to offer simultaneous functional-morphologic data without resorting to radiation, which is particularly desirable in pediatric patients.

Specific functional MRI techniques are Diffusion Imaging, MR Renography/Functional Urography, Blood-Oxygenation Level Dependent (BOLD) MRI, Renal perfusion MRI.

2.3.1 Diffusion Imaging

Diffusion is the process of thermally induced random molecular motion. Diffusion in biological systems is usually measured by the apparent diffusion coefficient (ADC), which includes contributions from factors such as perfusion. MR has proven to be the best method to measure water diffusion coefficients [11, 12].

Diffusion in the kidney is especially interesting to study because of its high blood flow and water transport function (Figure 2.4). Transport function in the nephrons and countercurrent mechanisms in the loop of Henle may have a substantial influence on the ADC values in the kidneys. Disease conditions such as acute tubular necrosis may cause alteration of water mobility in the kidneys. Diffusion imaging is a technique with unique contrast characteristics that could potentially provide information about microscopic tissue makeup. It is also sensitive to other microscopic and macroscopic transport mechanisms that may prove helpful in evaluating water transport in the kidneys both in healthy and pathologic states [4].

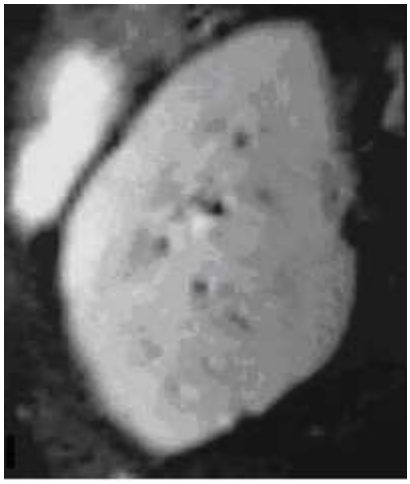

Figure 2.4 Sample of a diffusion-weighted image

2.3.2 MR Renography/Functional Urography

Functional MR urography, an analogue of the renal scan in nuclear medicine, could be used to evaluate split renal function. When combined with pharmacologic agents, captopril MR renography for evaluation of renal artery stenosis and diuretic MR urography to evaluate the significance of ureteral obstruction could be performed [4, 13]. MR renography is an extension of the first-pass perfusion imaging technique. Since most of the clinically approved MR contrast agents are gadolinium chelates that are excreted via the kidneys, temporal changes in the concentration of the agent within the kidneys can be monitored with MRI.

These temporal changes in concentration form the basis of conventional renography by nuclear medicine and hence it is possible to perform MR renography to evaluate renal function. The initial MR renography techniques have exploited the enhanced T2* due to concentrating effects of gadolinium chelates (Gd-DTPA) in the kidneys [14]. These techniques provided qualitative information on renal function, but were not quite amenable to quantitative analysis because of the complex interactions between T1 and T2* effects on the observed signal intensity [15].

2.3.3 BOLD MRI

It is known that oxyhemoglobin is diamagnetic and deoxyhemoglobin is paramagnetic [16]. Microscopic field gradients in the vicinity of red blood cells and vessels are modulated by changes in deoxyhemoglobin concentration. Such magnetic field perturbations within a voxel cause a loss of phase coherence and therefore lead to signal attenuation in gradient echo or T2* (apparent spin-spin relaxation time)-weighted sequences. This phenomenon is called blood oxygenation level dependent (BOLD) contrast [17].

Renal medullary hypoxia is believed to be an operative parameter in the pathogenesis of acute renal failure. BOLD MRI, a method widely used for functional MRI of the brain, is useful in the evaluation of intrarenal oxygenation. It allows understanding of the physiological factors that affect medullary hypoxia and hence, the pathophysiology of acute renal failure [4].

2.3.4 Renal Perfusion MRI

The Kidneys are the most highly perfused organ in the human body, handling about 20 % of the cardiac output or roughly 1.2 L/min. Lack of blood flow to the kidneys results in their failure to perform these important tasks and can lead to death within a few days due to inability to maintain homeostasis [5, 9].

If perfusion is compromised gradually over time, the overall renal perfusion can be initially maintained through counterregulatory mechanisms such as vasodilatation distal to the stenosis within the affected kidney. If the degree of stenosis exceeds a critical level (typically 70% are considered necessary), the perfusion pressure cannot be maintained and the development of arterial hypertension can ensue. This secondary type of arterial hypertension is thought to be present in approximately 5% of all patients with high blood pressure [18]. If a renal artery stenosis is severe enough to reduce renal perfusion below a critical perfusion level, renal blood flow further decreases and both glomerular and tubular function are reduced and permanent functional damage can occur. If renal perfusion is restored by means of revascularization procedures, these changes can be completely reversed.

Development of fast acquisition techniques provides sufficient temporal resolution to monitor intrarenal signal changes during the first pass of the agent through the kidneys (Figure 2.5). Renal perfusion MRI is able to image the kinetics of an exogenous contrast agent. Availability of an intravascular contrast agent facilitates acquisition of first-pass perfusion data. The first-pass perfusion technique which is used to obtain the renal perfusion data for this thesis work, involves bolus administration of an intravascular tracer and following its first pass through the kidneys, and the function of both kidneys can be characterized by qualitatively or semi-quantitatively analyzing the Signal Intensity-Time curves for the selected region of interest [19].

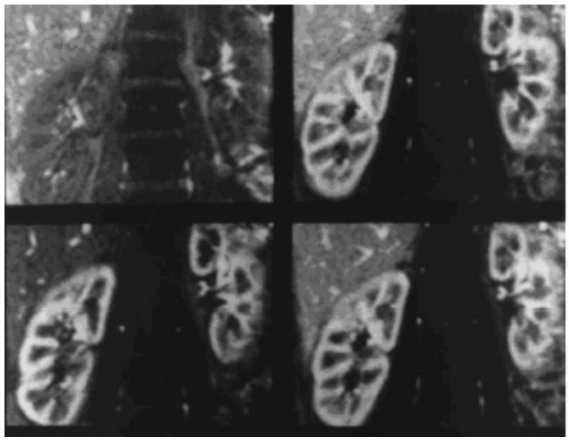

Figure 2.5 Sample perfusion images from the same slice

2.4 Contrast Agents in MRI

In spite of the excellent soft tissue contrast of MRI, the application of contrast enhancing agents in clinical MRI was proposed more than 15 years ago [20] and contrast agents are today an integral part of this image modality. MR contrast agent work by enhancing the relaxation rate of the protons in tissue, thereby altering the signal intensity in the image relative to areas not affected by the contrast agent. Knowledge of the relationship between contrast agent and MR signal response is an important requirement in contrast enhanced MRI in general and in MR based perfusion imaging in particular. This relationship is a complex function of the properties of the contrast agent as well as the structure of the target tissue and the imaging sequence.

A MR contrast agent can be thought of as a catalyst because in contrast enhancement MRI, the effect of the agent on proton relaxation is observed; not the contrast agent directly. MR contrast agents can be divided into different classes according to their magnetic properties relaxation and biodistribution. One of these classes contains the paramagnetic agents.

Paramagnetic agents contain water-soluble metal ions with or more unpaired electrons. The most common paramagnetic metal used as MR contrast agent is gadolinium (Gd^{3+}) which has seven unpaired electrons. For use, the gadolinium ions must be chemically linked to a carrier molecule, called a ligand, in order to reduce toxicity and alter the pharmacokinetic properties of the metal [20]. The resulting gadolinium containing molecule is referred to as a chelate, and currently available gadolinium based chelates are known as extracellular fluid (ECF) agents because they are distributed in the extracellular space following intravenous injection. Similar to inulin or iodine contrast agents, Gd chelates, such as Gd-DTPA, have a predominant renal elimination (around 98%) by glomerular filtration without tubular secretion or reabsorption [20]. Gadolinium-based contrast agents are widely used to increase the conspicuity of pathologic lesions of the kidney for MR imaging. These compounds are biologically inert, fully excreted by the kidneys, and handled physiologically in a manner similar to inulin.

3. MR RENOGRAMS

3.1 Introduction

In the dynamic MR procedure of the kidney, a slice is chosen that cuts through the kidney, and the contrast agent is injected intravenously. Care is taken to avoid saturation effects [15, 21], so that the image intensity is a measure of the contrast agent concentration and the uptake in and passage through the kidney of the agent can be interpreted. For this interpretation, the graphical displays (renograms) of the concentration of contrast agent in cortex and medulla as a function of time are used. Renograms are curves that show the contrast agent signal enhancement in the cortex and medulla of the kidney as a function of time and are an indicator of its function. To acquire MR renograms a series of dynamic Magnetic Resonance images is generated during and after a bolus injection of contrast agent. By recording the image intensity in the two tissues the renograms are recorded (Figure 3.1).

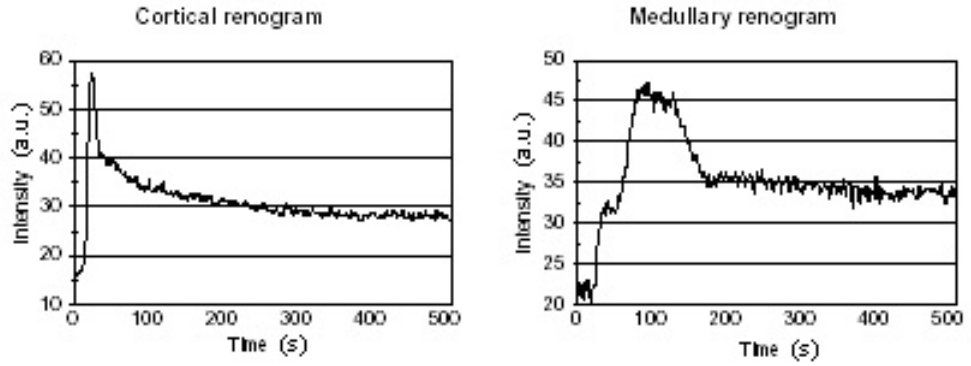

Figure 3.1 Cortical and medullary renogram

Potential advantages of MR renograms over scintigraphy are the higher spatial resolution of MR and the availability of cross section images instead of the projection images obtained via scintigraphy.

3.2 Partial volume effect

MRI makes images of a three dimensional volume, with as smallest unit the volume element (voxel). The pixels that can be viewed in images generated by an MRI scanner are two dimensional representations of these three dimensional voxels. The size of the voxels is determined by the operator of the MRI scanner. Its horizontal and vertical dimensions are equal to the size of the pixels. The pixel size is determined by the area of the field of view (for kidney images typically somewhere around 40 x 40 cm) and the image matrix size (typically 256 x 256). Voxel thickness is determined by the slice thickness setting (typically 8 mm). The signal to noise ratio of the voxel signal approximately increases linearly with the volume when all other parameters remain the same.

A problem with large voxels is that the volume they enclose can contain more than one tissue type, and the larger they become the larger the chance that this happens. This problem is called the partial volume effect. The different tissue types have curved borders and occupy limited volumes. For a given tissue type, its sensitivity for partial volume effects depends on these geometrical effects so the extent of partial volume effect depends on the dimensions of the voxel relative to those of the volume of the tissue of interest. In the dynamic scans, with a time resolution of 1.2 seconds, a slice thickness of 8 mm is considered to be minimally needed to obtain a decent image quality. Combined with the other two dimensions (1.6 x 1.6 mm) this results in a fairly tall voxel (Figure 3.2).

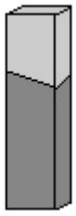

Figure 3.2 Schematic representation of a voxel with partial volume effect. The top of the voxel equals the pixel size. The height represents the slice thickness. The pixel intensity is a weighted average of the intensities of both tissues.

3.3 Cortical and Medullary Renograms

Low molecular Gd-DTPA diffuses fast into the extracellular space after an intravenous injection and it is immediately subject to renal excretion. This excretion is exclusively determined by the glomerular filtration without any tubular reabsortion. Because most of the water is reabsorbed in the tubulus a high concentration of Gd-DTPA may be reached in the medulla. Therefore, the cortical renogram can be considered as a reflection of the renal perfusion and a medullary renogram as a visualisation of the function of the nephron concerning its filter and reabsorption capacity.

By drawing region of interests (ROI's) that can be defined manually at direct selection of cortex and medulla over the cortex and medulla in the obtained images the signal intensity of the cortex and medulla can be calculated for each image. Analysis of the cortical contrast uptake enables to differentiate acute cortical necrosis which is not reliable possible with nuclear or ultrasound scans [13]. Similarly, analysis of medullary contrast uptake might facilitate the diagnosis of urinary tract obstruction and diseases primarily affecting the medulla [3].

3.3.1 Cortical Renograms

The cortex, which is responsible for distributing the blood over the kidney receives a bolus of the contrast agent and within a short time after arrival of the contrast agent at the kidney the concentration in the cortex reaches its maximum.

A high quality cortical renogram can be determined directly from a region of interest (ROI) placed in the cortex. Examination of the kidney shows that the outer layer of the kidney contains only cortical tissue. It also shows that increasing the slice thickness does not lead to the inclusion of other tissues in the voxels at the boundary of the cross-section if this cut is located at the broadest part of the kidney. Only when the slice thickness increases so much that the voxels leave the kidney, partial volume effect will occur.

3.3.2 Medullary (Cortica-Medullary) Renograms

The contrast agent reaches the medulla via a filtration process, which is relatively slow. Thus, when the contrast agent concentration in the cortex reaches its peak value, no contrast agent has yet entered the medulla. Any early enhancement of the pixels in a medullary region therefore will be due to the enhancement of cortical tissue that is present in the corresponding voxels.

Therefore covering only medullary tissue can in practice not be found, due to the irregular topology of the boundary between cortex and medulla, although in the MRI images a ROI that is only covering cortical tissue can be obtained reliably in the outer shell of the kidney [22]. This results in potential presence of cortical tissue in each of the voxels of the intended medullary ROI.

4. RENAL PERFUSION ANALYSIS

4.1 Introduction

MRI can characterize renal perfusion non-invasively with very high spatial resolution. In addition, it has the potential to simultaneously quantify perfusion of the kidneys using intra-vascular contrast agents, and blood flow through the renal arteries using phase-contrast imaging. Renal perfusion imaging using first-pass Gd-DTPA bolus has applications in studying renal vascular disorders, assessment of transplants, and screening and surgical planning [6].

Analysis of renal perfusion images entails several steps. For this thesis work, we integrated the necessary steps for renal perfusion analysis. These are as follows:

1. Importing Data: Images are browsed and loaded in DICOM (Digital Imaging and Communications in Medicine) format [23].

2. Image Display and Animation: The images are resized, zoomed, and adjusted for brightness and contrast to provide a uniform display of all frames.

3. Image Registration: Since the images often suffer from significant motion, prior to ROI analysis, it is necessary to align the images by correcting for this motion.

4. ROI Analysis: ROI-based analysis is performed by tracing ROI's and plotting time-intensity curves.

5. Perfusion Index Quantification: After identifying desired ROI's and characterizing the signal intensity versus time curves, it is desirable to quantify indexes such as slope, time-to-peak, and contrast enhancement ratio (CER).

4.2 The Flow of the Contrast Agent

The contrast agent is rapidly injected intravenously in the arm as a bolus. During its transport through the lungs, the heart and the aorta the bolus is only slightly diluted so that its concentration in the blood that enters the kidney still as a bolus, diminished in concentration and widened in time (10 s) due to diffusion of contrast agent in the blood. The Renal Perfusion MRI image series shows the following sequence:

- The vascular transit of the contrast agent lasts a few seconds, after which a peripheral cortical rim of high Signal Intensity (SI) is seen simultaneously in both kidneys as the contrast bolus arrives within the glomeruli.
- The subsequent homogenous increase and decrease in SI within the tissue reflects the contrast material uptake from the blood, and its later transport into the collecting system. When function is reduced in one kidney, tissue contrast enhancement is faint compared with the normal side. In some disease states the parenchyma may be narrowed eventually (dependent on the type of function reduction, acute or chronic) [19, 24].
- In the nonobstructed kidney, most of the contrast material is washed out by the time the study is completed. In the presence of relevant obstruction, the visually determined outflow from the renal pelvis is minimal or lacking.

4.3 Scanner Settings

During the scan, following intravenous bolus injection, the extracellular contrast agent Gd-DTPA enters the arterial space, the interstitium as well as the nephrons and increases the image intensity in both cortex and medulla. By placing separate regions of interest (ROI's) over renal tissues in each frame, signal intensity signals-time (TI-signals) are obtained. The temporal resolution (frame-to-frame time) of the scan is sufficient to resolve the events even during the fast arterial phase.

The scanner settings are limited by technological constraints. The presently used scan parameters are shown in Table 4.1.

Table 4.1
Scan Parameters

Scan method: 2D Spoiled Gradient Echo	Slice: 8 mm
Slice position: Through Long Kidney Axis	Number of slices: 6
Breathing instructions: Free Breathing	Frame time: 1.17 ms
Flip angle: 20^0	Number of frames: 80
Acquisition Matrix: 128 x 82 (Image Size: 256 x 256)	TR: 2.35 ms
Acquisition type: Multi-slice	TE: 1.15 ms

4.3.1 Slice Thickness

The information that can be retrieved from renograms depends on their signal to noise ratio (SNR), which can be increased by increasing the slice thickness. However, when the slice thickness increases, it can be expected that the fraction of cortical tissue present in the ROI selected in the medullary region will increase as well. As mentioned before, the outer region of the kidney contains only cortical tissue so a pure cortical TI signal can be easily obtained. When the slice thickness becomes too large the curvature of the kidney's circumference becomes an issue. Tall voxels in this region could leave the cortex and include other tissues. For this reasons there is a limit for slice thickness.

4.3.2 Single or Multi Slice

By using multi slice imaging, through slice movement induced noise should be strongly reduced. This is because the spins in multiple slices are saturated, and, except for the outer slices, when through slice movement is present, the saturated spins that are moved out of the slice are replaced with other equally saturated spins. The reduction depends on the slice distance and potentially on the slice profile.

The strong through plane movement that occurred between the single slice images has caused a considerable increase in brightness in the latter image. This increase is particularly clear in the fat tissue below the kidney, but also intrarenal pixel intensity changes can be seen (Figure 4.1). There is through plane movement also in multi-slice images, however breathing period is more easily recognisable in the single slice scan [25].

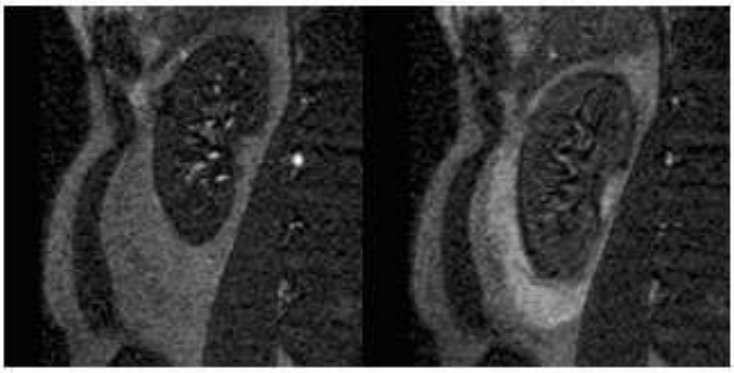

Figure 4.1 Pixel intensity changes in and around the right kidney in a single slice scan. Shown are the normal pixel intensities (first image) and the pixel intensities just after end inhalation (second image).

Figure 4.2 shows an example images of two slice locations from a patient with renal cysts [25]. The lack of enhancement in the cysts corroborates the non-cancerous nature of the lesions. The cyst, seen in the left kidney in Figure 4.2a, is not readily apparent in the adjacent slice shown in Figure 4.2b, underscoring the importance of a multi-slice acquisition.

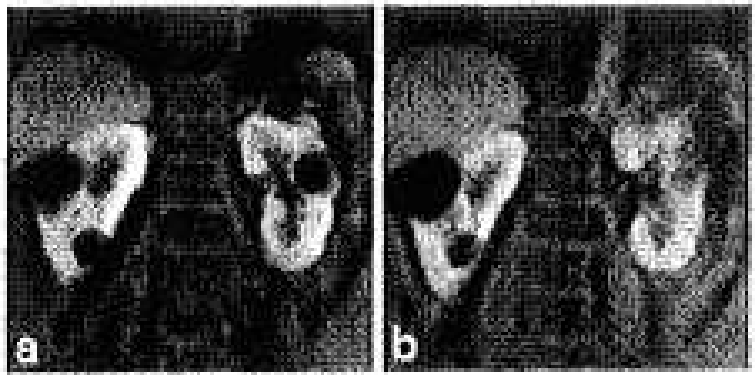

Figure 4.2 Patient with renal cysts. Two perfusion images from contiguous slices

4.3.3 Slice Orientation

Kidney movement due to respiration of the native kidney is approximately a translation. Kidneys are located close to the musculus erector spinae and the plane of movement of the kidney is parallel to the surface of this muscle as shown in Figure 4.3. The three lines have exactly the same location in both images. Via the two long lines the movement of the kidney can be observed while the small line between kidney and musclulus erector spinae shows that the distance between those two remains constant. This means that through plane movement can be reduced effectively by selecting a slice orientation parallel to the movement direction.

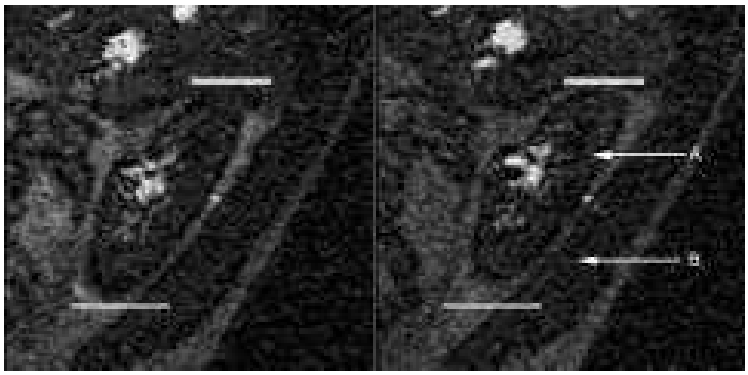

Figure 4.3 Movement of the Kidney. The three lines have exactly the same location in both images. Via the two long lines the movement of the kidney can be observed while the small line between kidney and musclulus erector spinae shows that the distance between those two remains constant. The arrows indicate the kidney (A) and the musclulus erector spinae (B).

4.4 Image Registration

To plot signal intensity-time curves of the cortical and medullary regions, ROI's are placed on the kidney in images acquired using dynamic MRI. The signals were recorded from ROI's that were automatically copied after manual segmentation of one of the images early in the dynamic series.Since native kidneys move with breathing and breath holdingtechniques are not feasible (moreover, it has been shown [26] that even during breath holding the diaphragm is not motionless), movement correction is necessary.

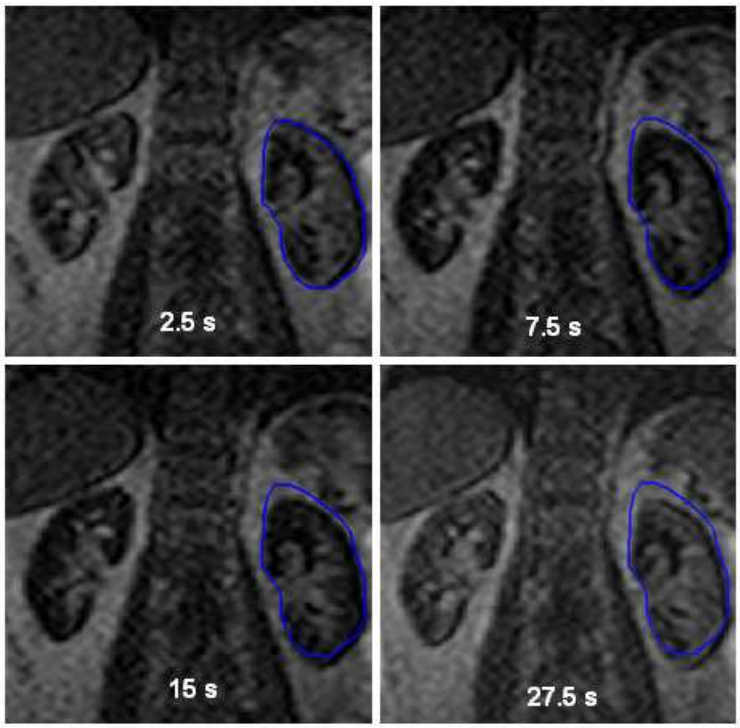

Figure 4.4 The motion of the kidney positions in 4 adjacent scans. The selected region is exactly the same in all images.

The first-pass transit of contrast agents is typically imaged over 60 - 90 sec, which is too long for a breathhold. Thus, in perfusion imaging and other such applications, it becomes imperative to correct the misalignment of the images by registering them prior to their use for quantification. Fortunately, the breathing movement does not cause appreciable rotation or distortion of the kidney so that in a suitably angulated coronal plane the kidney cross-section in the images has a constant shape. It is shown that the movement of the kidney due to breathing results in a Head to Feet (HF) shift that is normally well within 10 pixels, although slightly larger values sometimes occur [27]. The Left to Right (LR) shift is in most cases zero or one pixel (Figure 4.4).

An adequate movement correction can be performed by only shifting the image. It is possible to perform this shifting manually, but given the large number of scans used for the signal intensity-time curves, that is a time consuming job. To automatically measure signal intensities in dynamic MRI studies when motion is present, a method is therefore needed to automatically retrieve the kidney position in each scan.

Our image registration algorithm [28, 29] is to compensate the image misalignment due to breathing. The employed algorithm and the source code in (ANSI) C are freely downloadable [29]. It is utilized as a dynamically linked ".dll" to MATLAB using "Mex" interface. The algorithm performs a sub-pixel registration that minimizes the mean square intensity difference between the two images to be registered by using a variation of the Marquardt-Levenberg nonlinear least squares optimization. In order to improve speed and convergence the algorithm uses an iterative coarse-to-fine pyramid approach and it uses cubic spline interpolation for image transformation.

The registration process starts with the first image in the series. A selected region forms the mask. The optimum displacement amount is computed within this search region. The second image is then translated by the computed displacements to align it spatially with the first image. This process is repeated for all pairs of images in the series. Figure 4.5 and Figure 4.6, respectively, show an example of the signal intensity-time curves obtained from unregistered and registered renal perfusion images. The selected regions are same for registered and unregistered images.

4.5 Region of Interests (ROI's)

Region of interests (ROI's) are used to extract functional information. A ROI is a closed contour placed over the image and defines an area which can be used for calculating statistics. These measurements include, but are not limited to, surface area, average pixel intensity of all the pixels enclosed by the ROI and the standard deviation of these pixel intensities.

In dynamic MR of a non-moving tissue, a ROI is placed over the tissue of interest in one image and copied to all the other images. This makes it possible to measure the average pixel intensity of the tissue during a scan. In combination with a contrast agent this allows to a record of the history of the contrast agent concentration in that tissue.

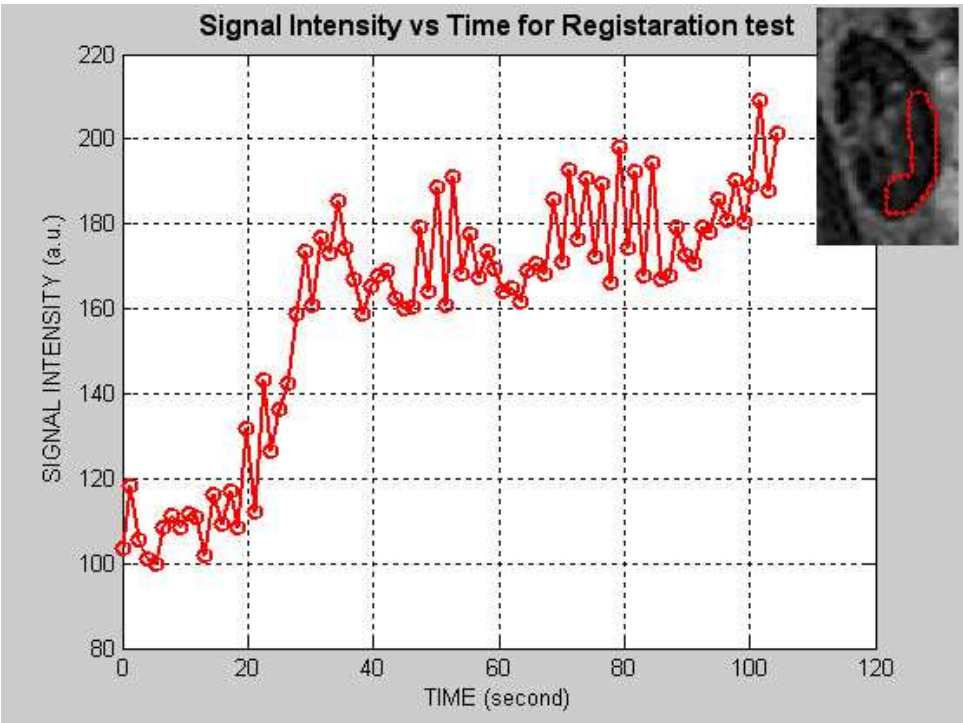

Figure 4.5 An example of the signal intensity-time curves which obtained from unregistered renal perfusion images

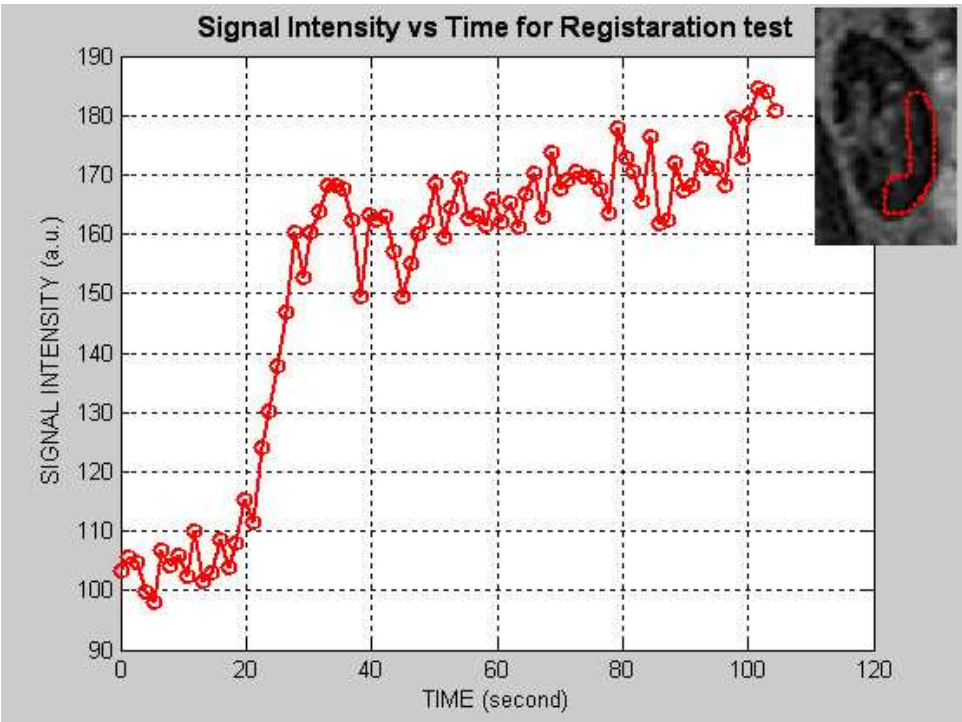

Figure 4.6 An example of the signal intensity-time curves which obtained from registered renal perfusion images (ROI is the same as in Figure 4.5.)

The outer 5 millimeter of a kidney includes cortical tissue only whereas the remaining more central located renal parenchyma includes both cortical and medullary tissue. Therefore signal intensities of a region of interest in the central located renal parenchyma after injection of an MR contrast medium provide a mixture of cortical and medullary signals.

4.5.1 ROI's on the Cortical Region

ROI selection on the cortical region at the periphery of the kidney is easy, because this region is free of medullary tissue. Based on the assumption that the outer layer of the kidney only contains cortical tissue, a cortical ROI can be drawn in the strongly enhanced images (Figure 4.7).

4.5.2 ROIs on the Medullary Region

The complex-shaped medullary pyramids border the cortical tissue throughout the kidney many voxels contain a mix of cortical and medullary tissue. As mentioned before, in the individual images of the dynamic MRI scans cortical and medullary renal tissue are often hard to differentiate and computer based segmentation of these tissues has thus far not been possible (Figure 4.8).

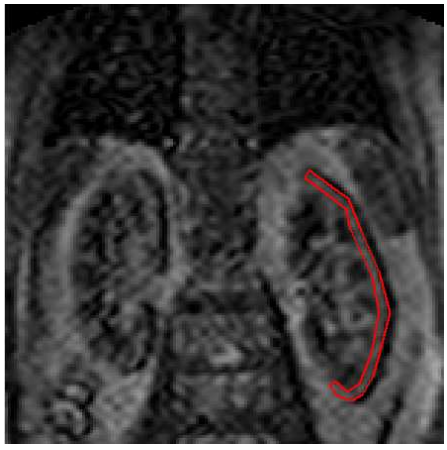

Figure 4.7 ROI on the cortical region

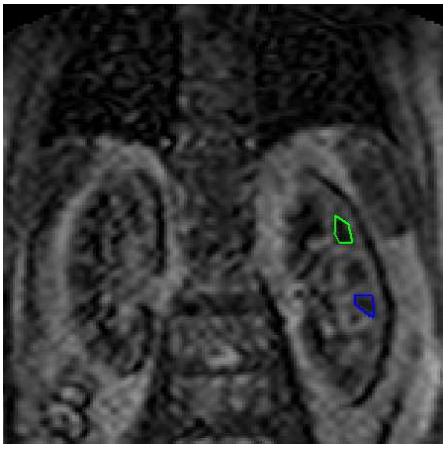

Figure 4.8 ROI's on the medullary region

Since the microvascular system of the medulla is connected in series with that of the cortex, the contrast agent arrives later in the medulla than in the cortex. Therefore, the initial period of the mixed signal contains only cortical signal [30, 31].

4.6 Perfusion Indexes

The last process of the Renal Perfusion Analysis is to plot the Signal Intesity-Time Curve and compute slope, time-to-peak, and contrast enhancement ratio (CER) from this curve.

By determining the average pixel intensity in the ROI's (the sum of the intensities of all pixels in the ROI divided by the number of pixels in that ROI) and repeating this for all images, time-dependent signals are generated. The average pixel intensity values are used to plot the Signal Intensity-Time Curve. At the end, the indexes such as slope of the first-pass enhancement, time-to-peak, and contrast enhancement ratio for both left and right kidney ROI's are computed.

The steps are the following:

- Taking the signal intensity-time curve data and smoothing the curve to get rid of the effects of noise. MATLAB's smoothing algorithm with "moving average filtering method" is proper option for this step. A moving average filter smooths data by replacing each data point with the average of the neighboring data points defined within the span. This process is equivalent to lowpass filtering with the response of the smoothing given by the difference equation:

$$y_s(i) = \frac{1}{2N+1}(y(i+N) + y(i+N-1) + ... + y(i-N)) \tag{4.1}$$

where y_s(i) is the smoothed value for the ith data point, N is the number of neighboring data points on either side of y_s(i), and 2N+1 is the span.

- Calculating the first derivatives of this smoothed curve pointwise, and finding the maximum of the first derivatives. This is the maximum slope (m_{max}) in the data.

The slope (m) is:

$$m = \frac{S_{peak} - S_{arrival}}{t_{peak} - t_{arrival}} \tag{4.2}$$

The Contrast Enhancement Ratio (CER) is:

$$CER = \frac{S_{peak} - S_{baseline}}{S_{baseline}} \tag{4.3}$$

Setting a threshold equal to 10% of the maximum slope and searching the first derivatives earlier than the time of maximal slope for where the slope first becomes larger than this threshold. This time point is considered as the arrivaltime ($t_{arrival}$), and the signal intensity at this time is the arrivalsignal ($S_{arrival}$). Similarly, searching the first derivatives after the time of the maximal slope, and finding the time point where the slope first falls below the threshold. This is considered the peaktime (t_{peak}) and the signal here is considered as the peaksignal (S_{peak}). $S_{baseline}$ is baseline signal. It is obtained by averaging all the points before the arrivaltime ($t_{arrival}$). Figure 4.9 and Figure 4.10 show an example curve obtained from the cortical region and parametric images of indexes.

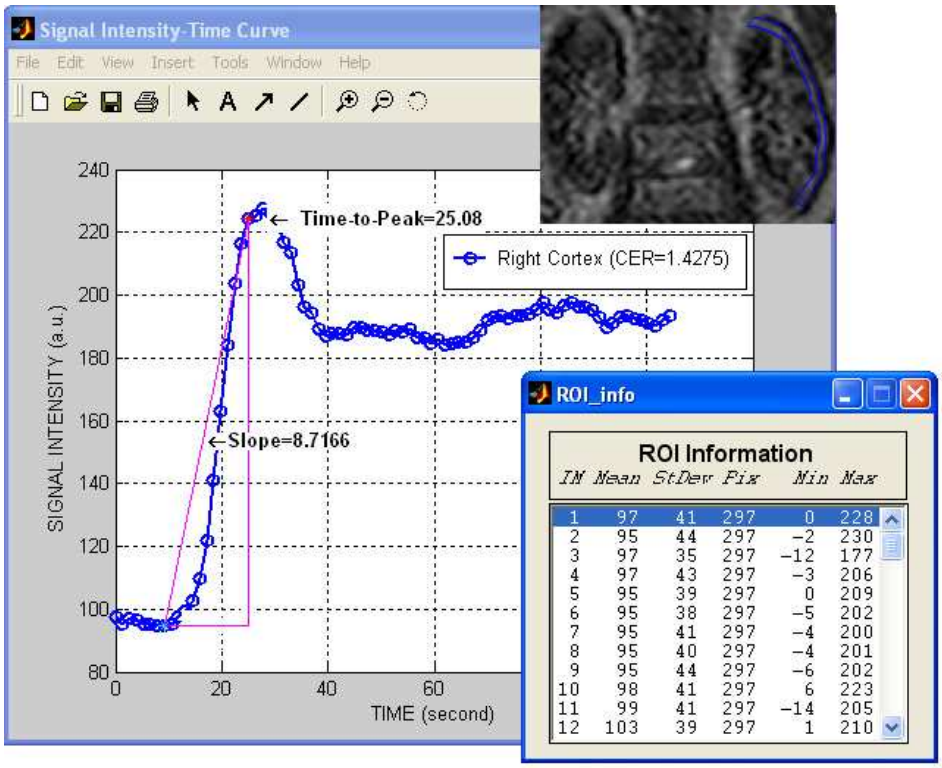

Figure 4.9 Sample Signal Intensity-Time Curve and its indexes

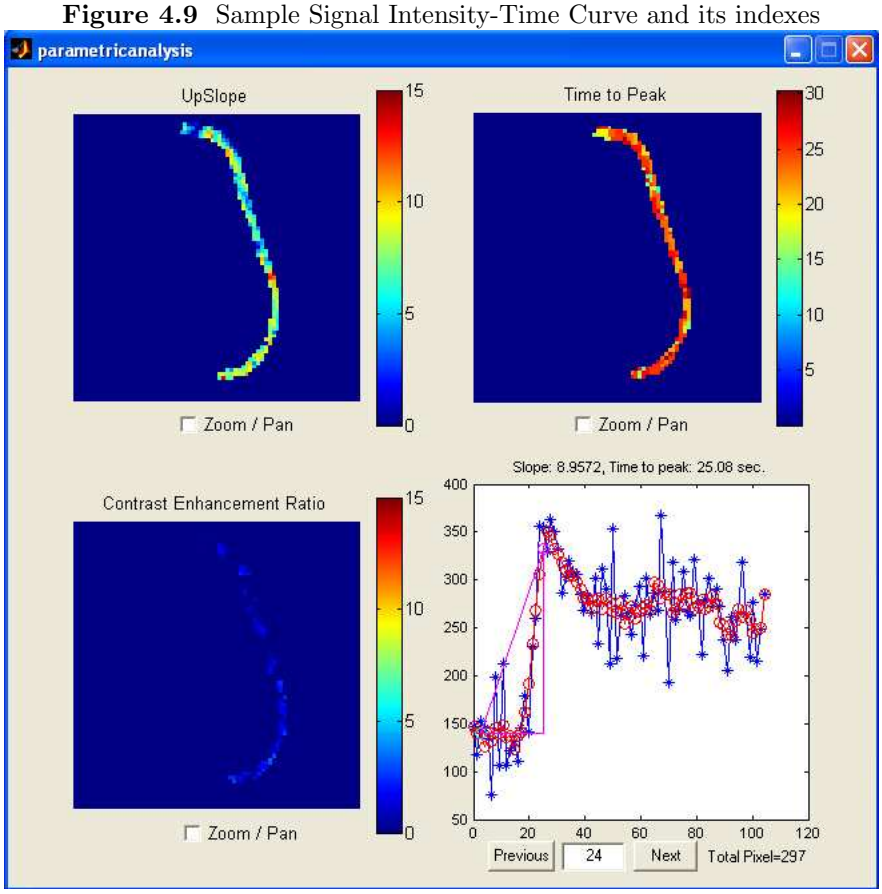

Figure 4.10 Sample Parametric Images of the Renal Perfusion indexes

5. ANALYSIS RESULTS

5.1 Introduction

Our MATLAB program is tested to analyze renal perfusion data which obtained from 10 volunteers (Table 5.1) who were patients undergoing MR exam with contrast administration for other reasons.

All volunteers had normal renal function. In this chapter, the results of the analysis are presented individually and in detail.

Table 5.1
Age and Sex of the Volunteers

Volunteer	Age	Sex
1	74	Male
2	44	Female
3	66	Male
4	51	Female
5	71	Male
6	46	Female
7	43	Female
8	46	Female
9	70	Male
10	75	Male

5.2 Methods

For renal perfusion imaging using first-pass Gd-DTPA bolus, the MR examinations were made with a Philips Intera Scanner (1.5T, slewrate 150 mT/m/ms, maximal gradient strength 30 mT/m, Philips Medical Systems) and included a dynamic first pass renal scan.

For this dynamic scan we used T1-FFE (Fast Field Echo) sequence (TR=2.35ms, TE=1.15ms, flip angle=20^0) with a 400 mm field of view and a slice thickness of 8 mm. The resolution is 256 x 256 pixels. We obtained 80 images for each of the six coronal slices through the kidney, with a frequency of about 1 image per 1.35 seconds. The contrast agent Gd- DTPA was injected manually (To prevent saturation we used low dose (1.5-2 cc) of contrast agent.) before scan starts. We verified that 80 (480/6) images suffice to record the major signal changes related to the first pass of the agent. All examinations were stored on CD ROM's and transported to a personel computer for analysing with our analysis tool.

5.3 Results

The dynamic MRI image series shows the following: The vascular transit of the tracer lasts a few seconds, after which a peripheral cortical rim of high SI is seen simultaneously in both kidneys as the contrast bolus arrives within the glomeruli. The subsequent homogenous increase and decrease in SI within the tissue reflects the contrast material uptake from the blood, and it's subsequent transport into the collecting system.

By performing dynamic MRI during the injection, the transit of the contrast medium through the kidney can be followed. Qualitative assessment of the renal function by this method shows differences in the curves pattern between well-functioning kidneys and pathologic kidneys. Differences from the normal response profile can be observed in ischemic, renal failure, and after renal transplantation [32]; however, the analysis is qualitative or semi-quantitavive using parameters such as the maximum of the renal peak or the slope of the wash in. It has not been possible to establish generally acceptable normal values for most of these parameters, which can be transferred from one study to another. The main reason for this is the inconstant and nonlinear relationship between Gd-DTPA tissue concentration and SI, which varies between specific MRI techniques used depending on the hardware as well as on the sequence used. The injection speed of the contrast medium and cardiac output are another reasons.

In MRI, the relationship between Gd-DTPA tissue concentration and the measured SI is usually non-linear since the intensity of the MR signal is a complex function of the gadolinium tissue concentration, which is dependent on magnetic field strength, gradient strength, sequence parameters, magnetic susceptibility, and on the amount of the contrast agent.

The renal perfusion gradually decreases from the outer cortex to the inner medulla. Because age and essential hypertension decrease the renal blood flow, the relative low value of the cortical blood flow can be observed in well-functioning native kidneys. The delay of cortical time to peak is indicative of altered renal perfusion and appears to be of clinical value in differentiating vascular from glomerular nephropathies.

Using our protocol, a constant pattern of enhancement was noted in the cortical ROI's. As expected in normal volunteers, the renal cortex enhanced vividly within the first 10-20 s following injection of the contrast agent. The maximal signal intensity occurs at approximately 15-30 s after the first signs of Gd-DTPA arrival in the cortex. This peak is followed by a slow constant drop in signal intensity, reflecting the onset of glomerular filtration and dilution in the extravascular space.

The functional parameters obtained from ten volunteers with normal renal function are shown in (Table 5.2). In the following pages, figures of the selected region of interests with theirs SI-Time curves and functional parameters and the histogram graphs of Slope, Time-to-peak and CER values of pixels inside left and right cortex are also shown for each volunteer.

From these results, we concluded that, the time-to-peak values are nearly the same, whereas the slope and CER indexes have different values for both kidneys of each volunteer. Because of the different location of the kidneys, the Signal Intensity-Time curves of left and right cortex have different baseline signal.

Table 5.2
Indexes from SI-Time Curves

No	Kidney	Slope	CER	Time-to-Peak
1	Left	6.06	1.14	31.50
	Right	5.65	0.98	32.76
2	Left	6.19	0.89	22.50
	Right	5.66	0.85	22.50
3	Left	9.67	1.72	20.80
	Right	7.38	1.04	20.80
4	Left	5.07	0.92	30.00
	Right	4.58	0.71	28.75
5	Left	5.76	1.36	18.34
	Right	4.43	0.65	18.34
6	Left	11.80	1.1	23.94
	Right	11.15	1.01	23.94
7	Left	11.34	0.55	20.96
	Right	8.82	0.46	20.96
8	Left	11.55	1.94	21.25
	Right	9.49	0.62	20.00
9	Left	6.55	1.31	27.72
	Right	5.47	0.96	27.72
10	Left	4.13	1.34	30.36
	Right	3.51	0.74	30.36

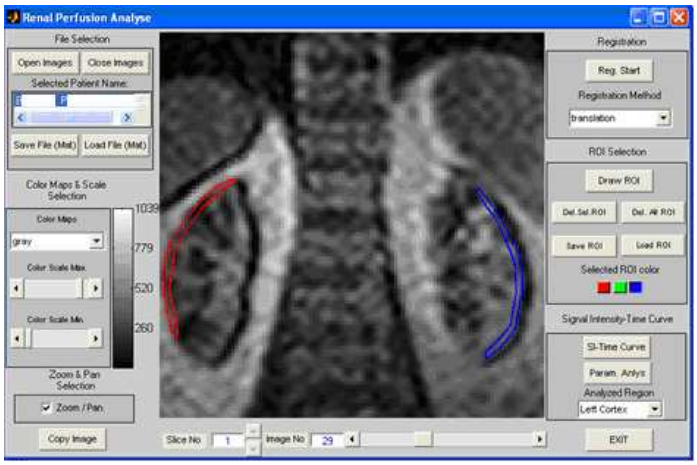

Figure 5.1 ROI's for Volunteer 1

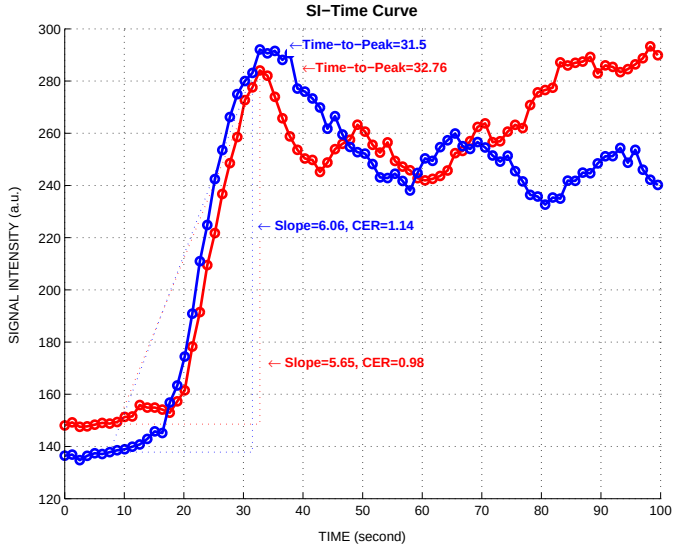

Figure 5.2 SI-Time Curve for Volunteer 1

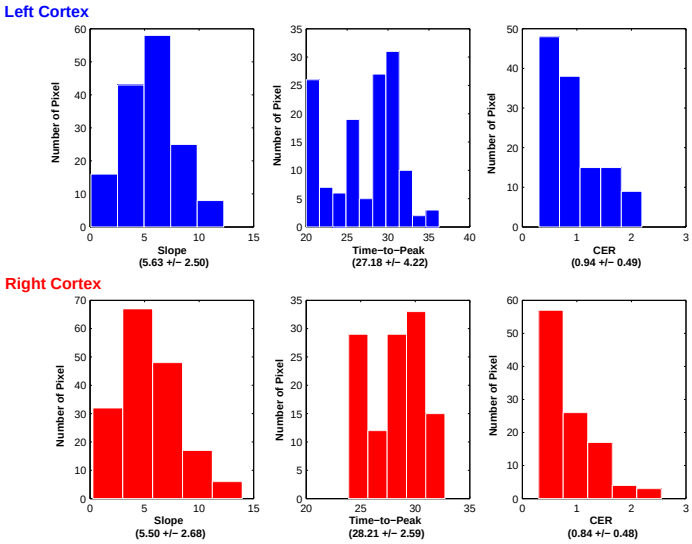

Figure 5.3 Histogram Graphs of Slope, Time-to-peak and CER values of pixels in the selected ROI's

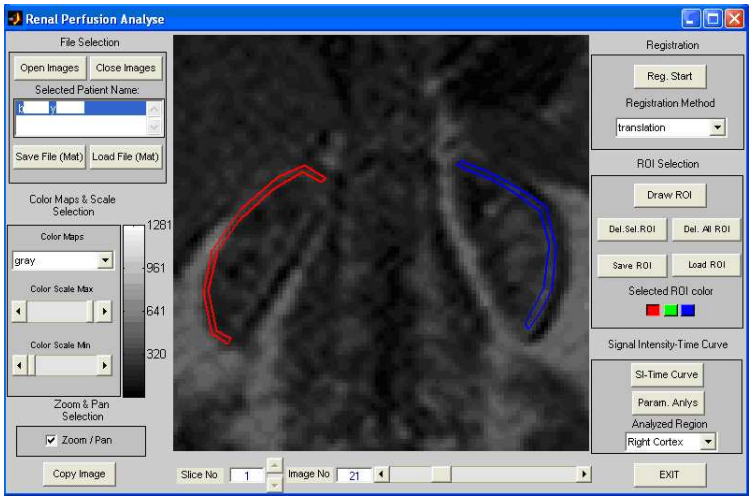

Figure 5.4 ROI's for Volunteer 2

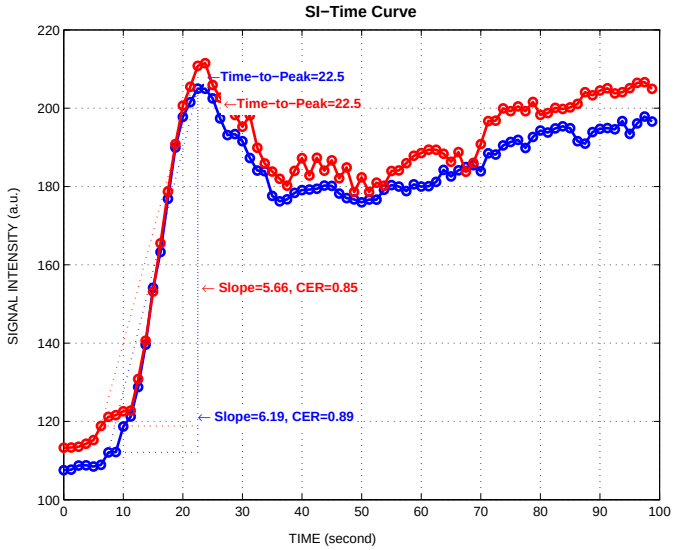

Figure 5.5 SI-Time Curve for Volunteer 2

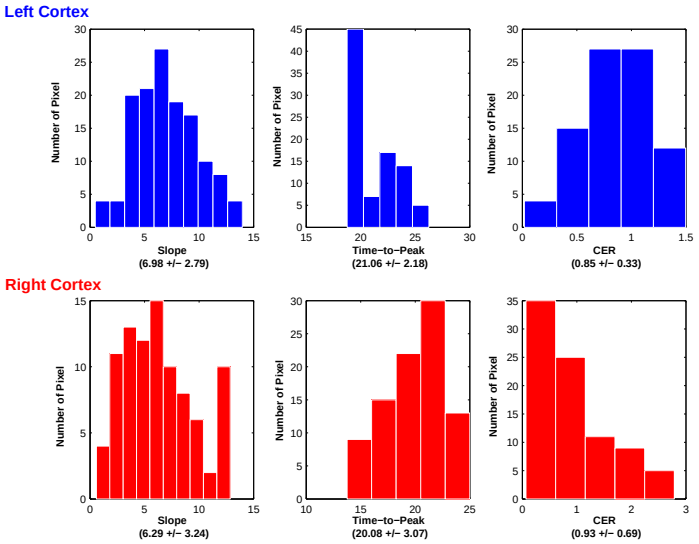

Figure 5.6 Histogram Graphs of Slope, Time-to-peak and CER values of pixels in the selected ROI's

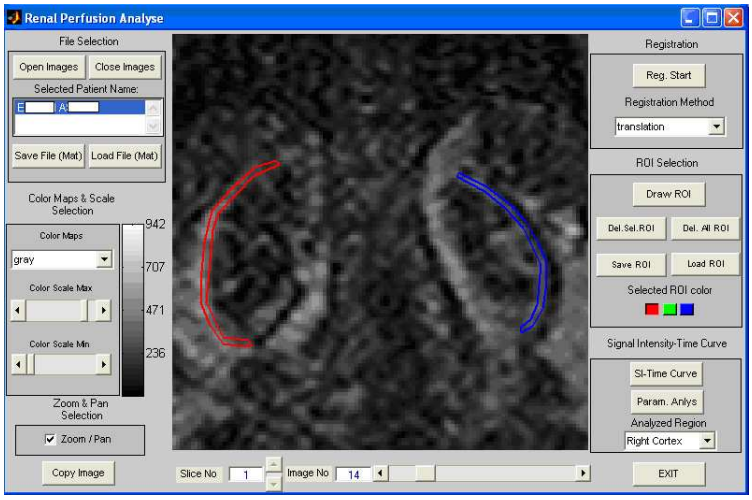

Figure 5.7 ROI's for Volunteer 3

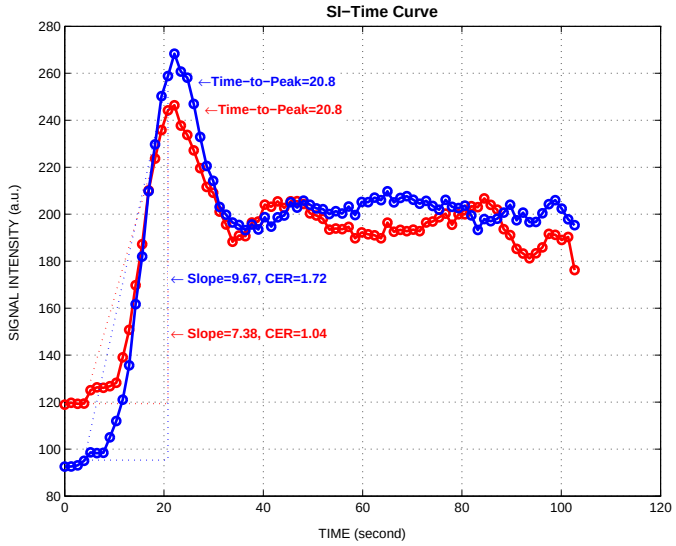

Figure 5.8 SI-Time Curve for Volunteer 3

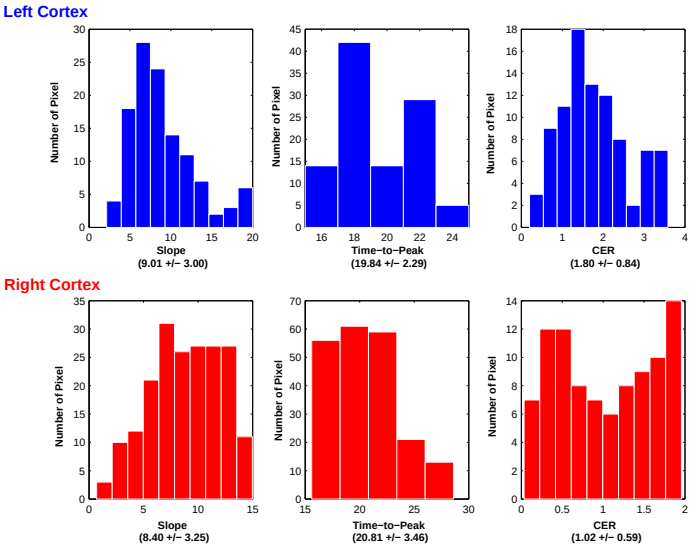

Figure 5.9 Histogram Graphs of Slope, Time-to-peak and CER values of pixels in the selected ROI's

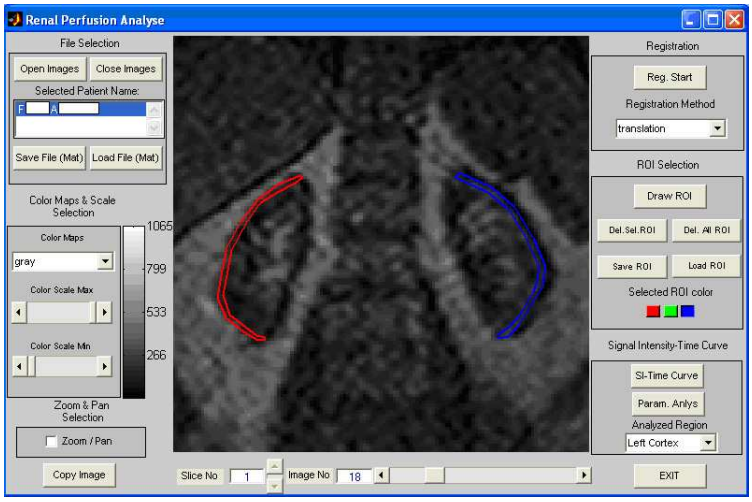

Figure 5.10 ROI's for Volunteer 4

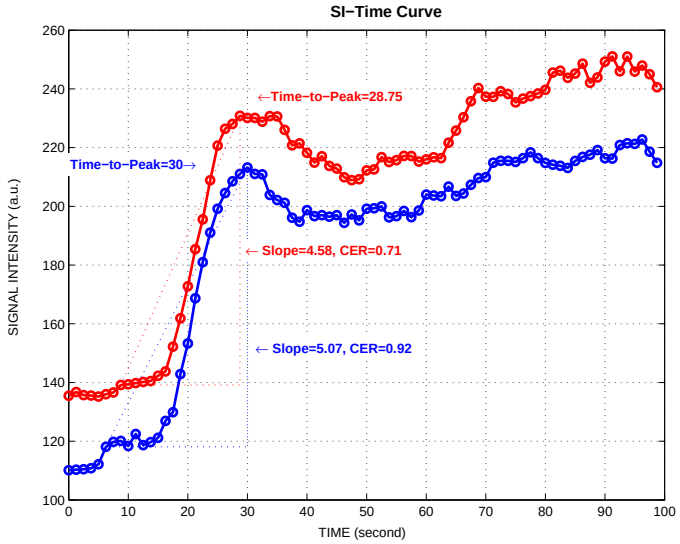

Figure 5.11 SI-Time Curve for Volunteer 4

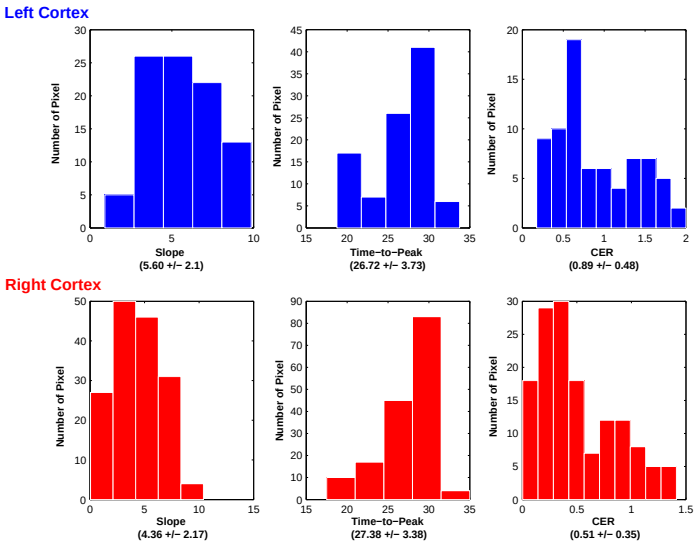

Figure 5.12 Histogram Graphs of Slope, Time-to-peak and CER values of pixels in the selected ROI's

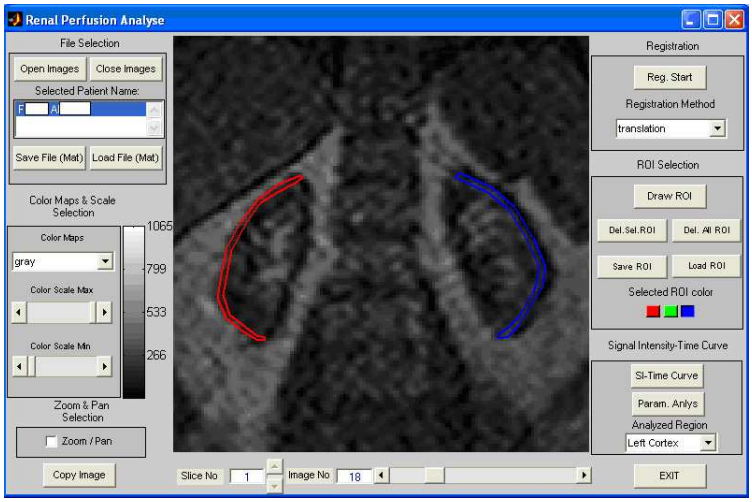

Figure 5.13 ROI's for Volunteer 5

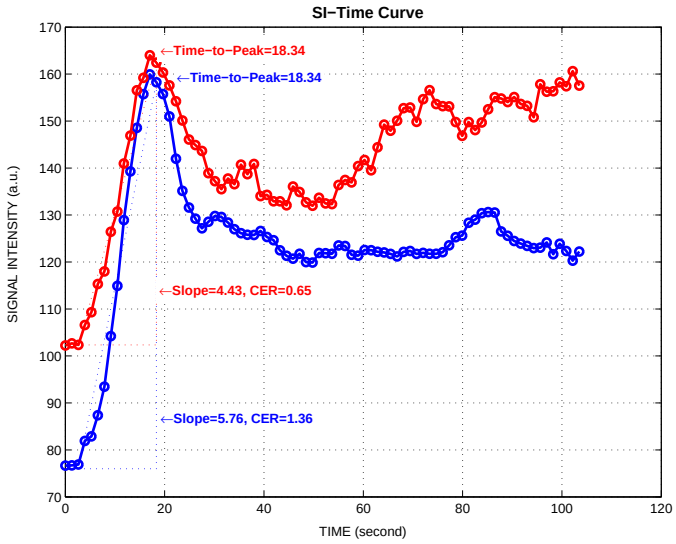

Figure 5.14 SI-Time Curve for Volunteer 5

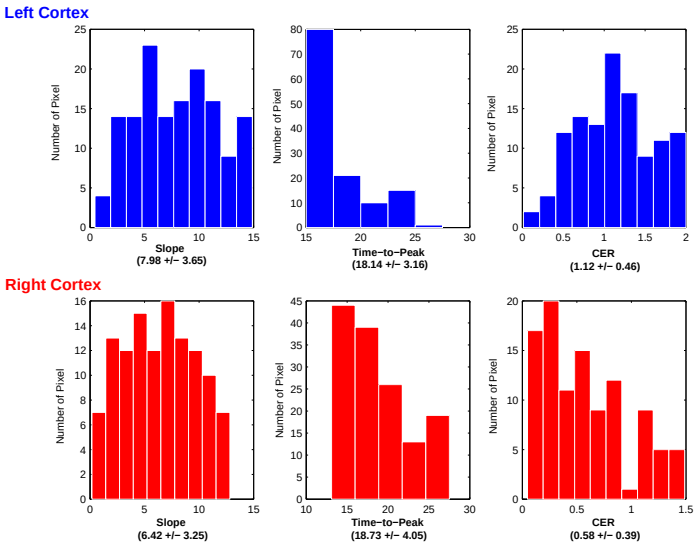

Figure 5.15 Histogram Graphs of Slope, Time-to-peak and CER values of pixels in the selected ROI's

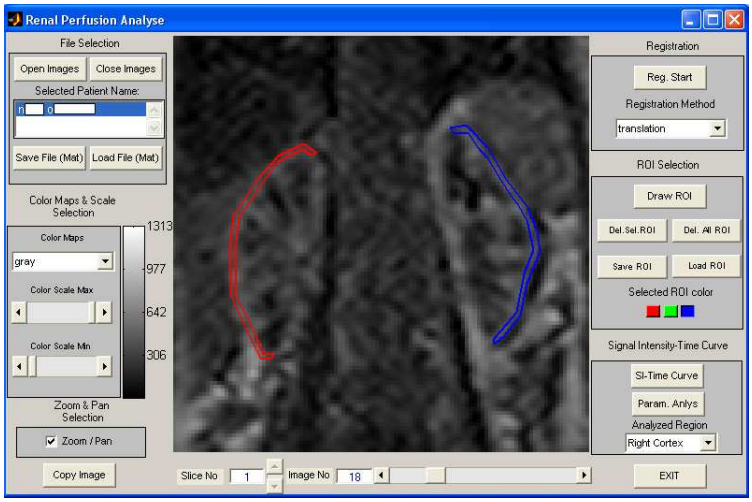

Figure 5.16 ROI's for Volunteer 6

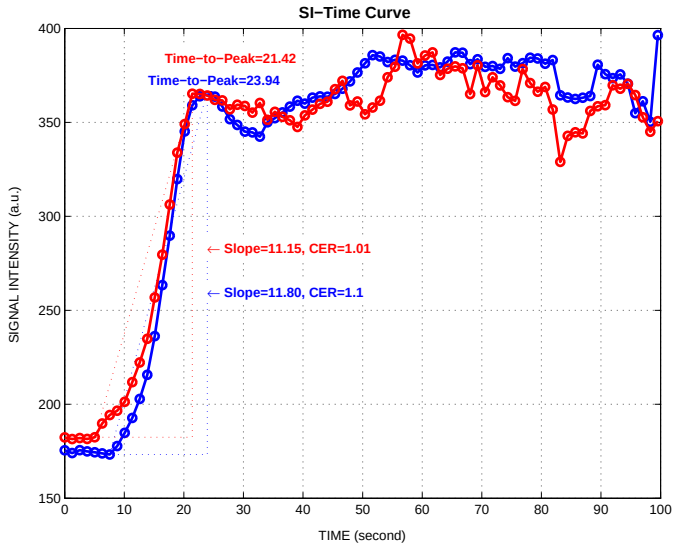

Figure 5.17 SI-Time Curve for Volunteer 6

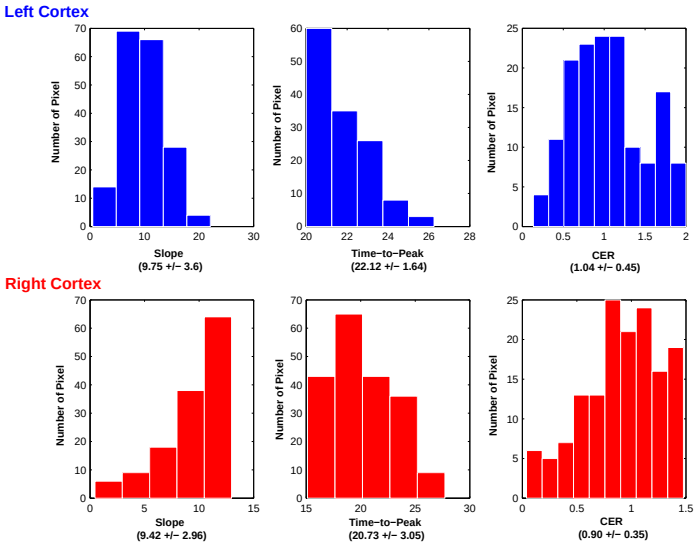

Figure 5.18 Histogram Graphs of Slope, Time-to-peak and CER values of pixels in the selected ROI's

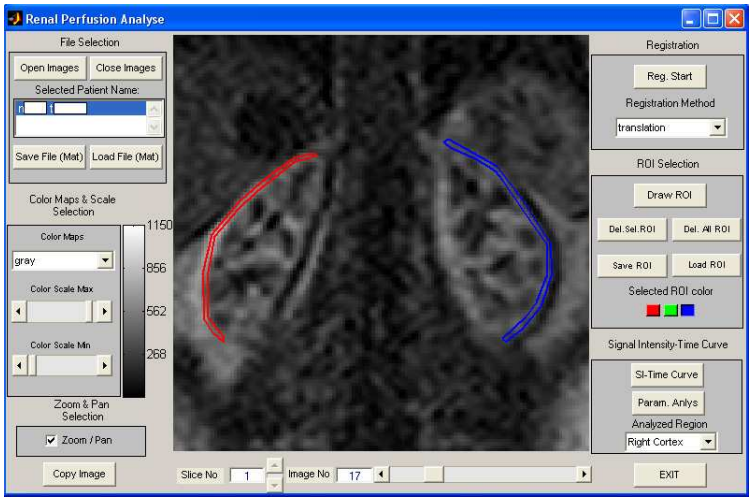

Figure 5.19 ROI's for Volunteer 7

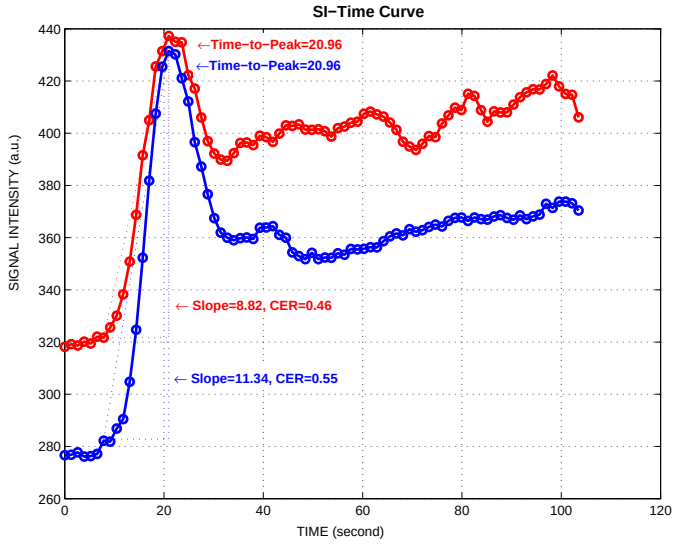

Figure 5.20 SI-Time Curve for Volunteer 7

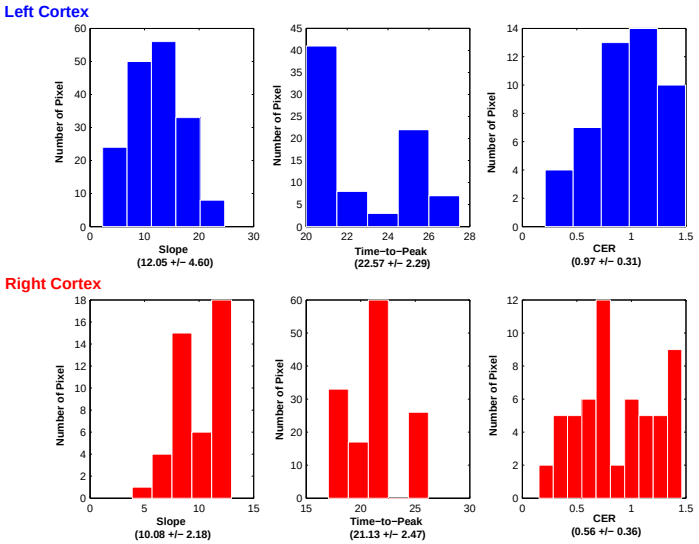

Figure 5.21 Histogram Graphs of Slope, Time-to-peak and CER values of pixels in the selected ROI's

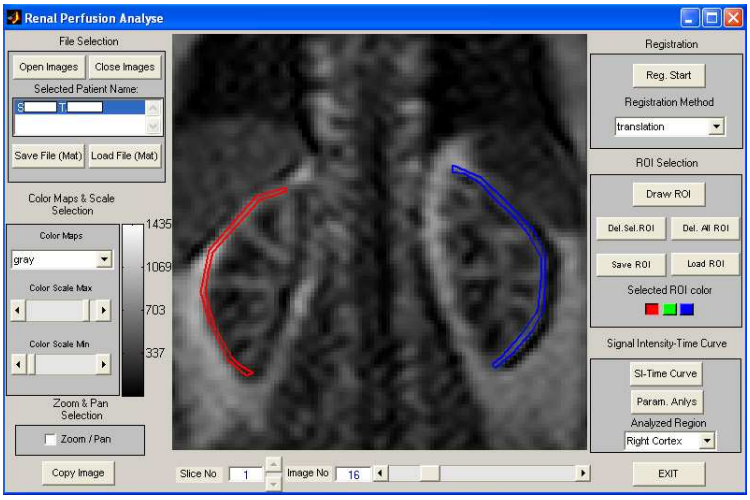

Figure 5.22 ROI's for Volunteer 8

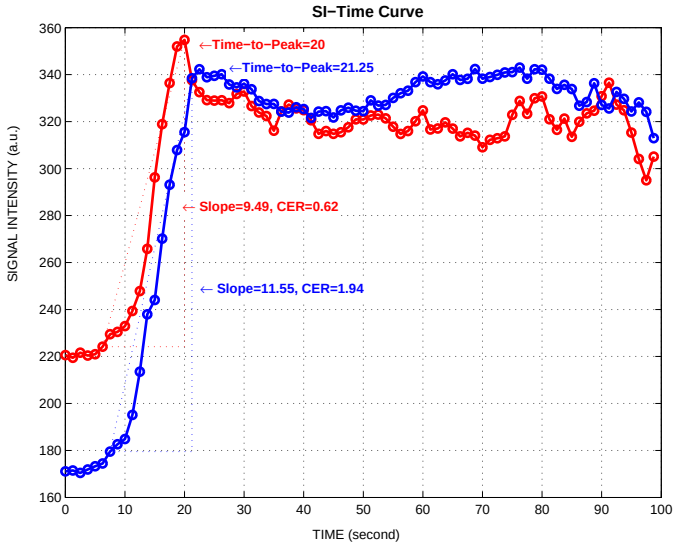

Figure 5.23 SI-Time Curve for Volunteer 8

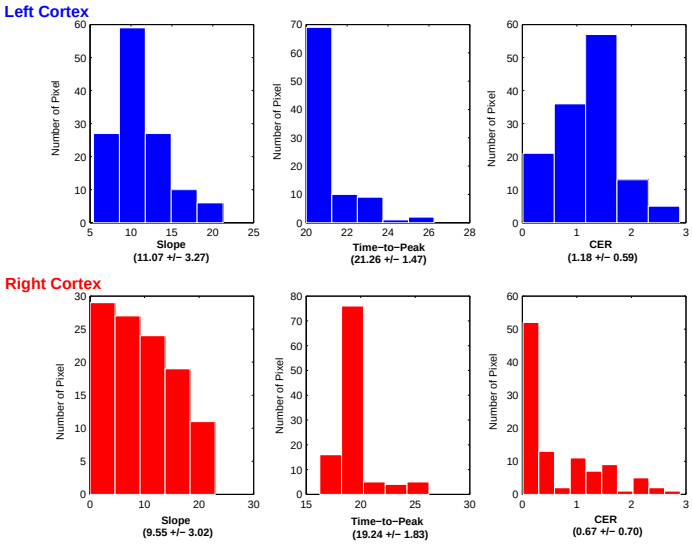

Figure 5.24 Histogram Graphs of Slope, Time-to-peak and CER values of pixels in the selected ROI's

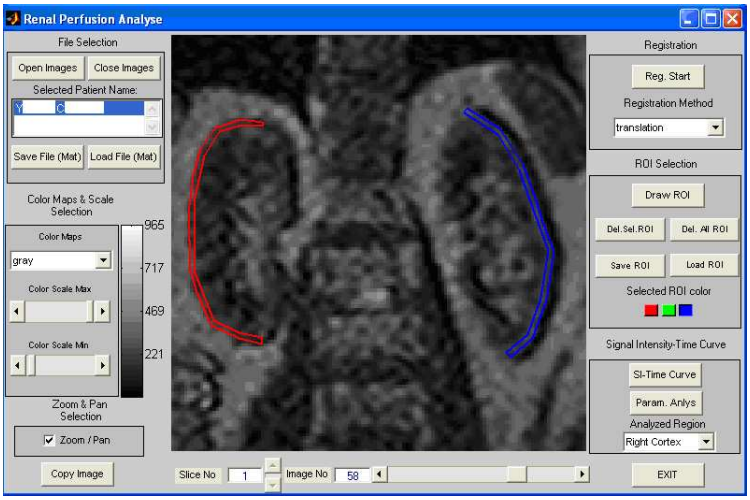

Figure 5.25 ROI's for Volunteer 9

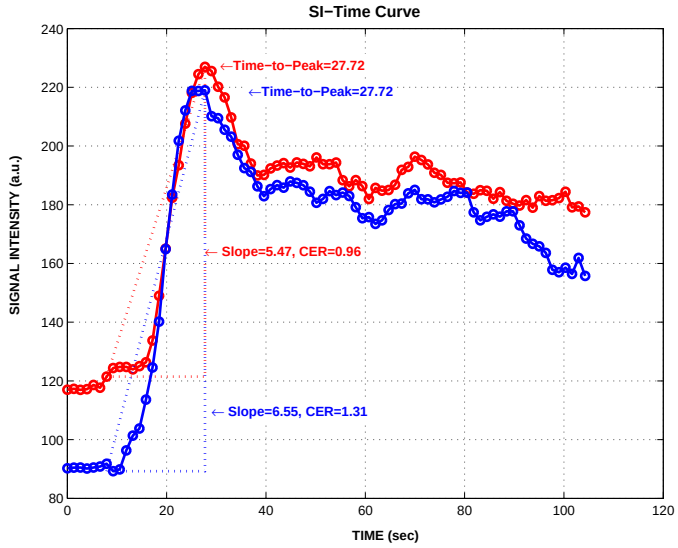

Figure 5.26 SI-Time Curve for Volunteer 9

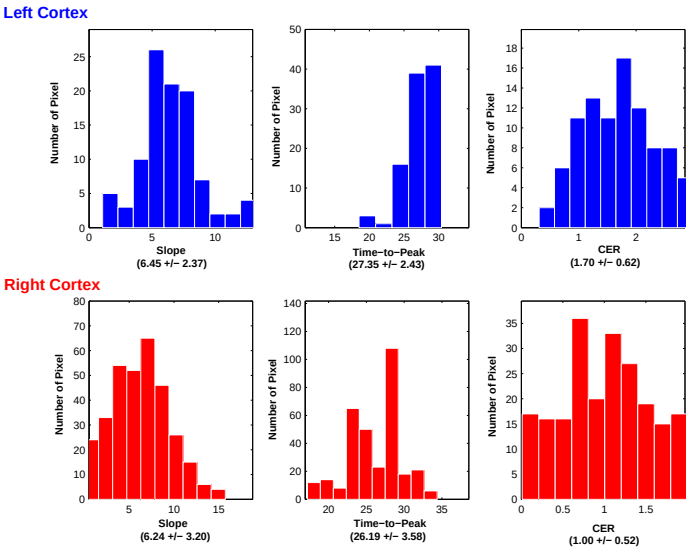

Figure 5.27 Histogram Graphs of Slope, Time-to-peak and CER values of pixels in the selected ROI's

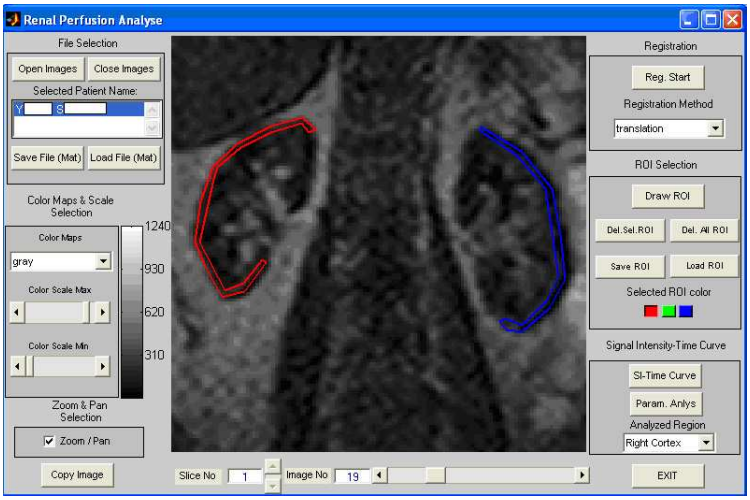

Figure 5.28 ROI's for Volunteer 10

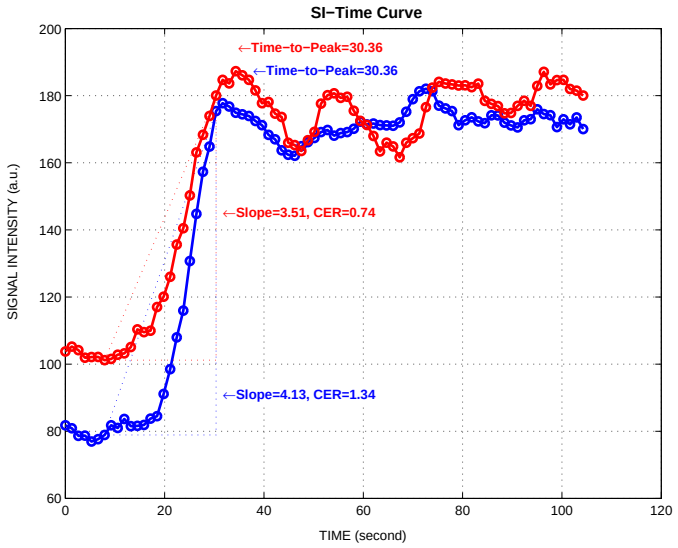

Figure 5.29 SI-Time Curve for Volunteer 10

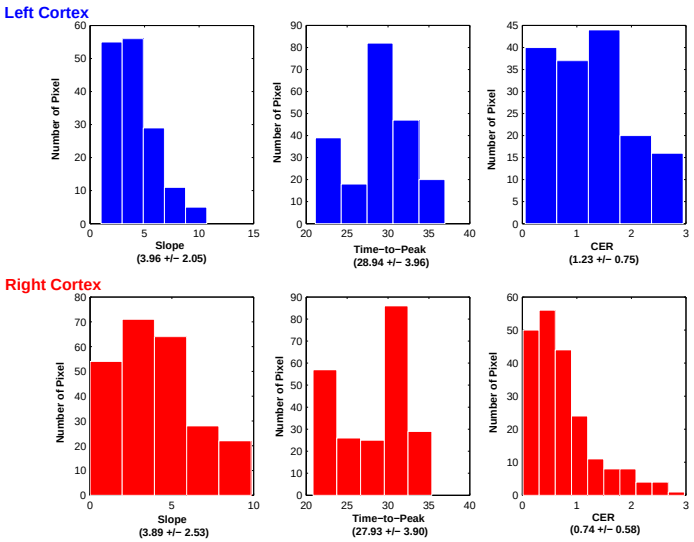

Figure 5.30 Histogram Graphs of Slope, Time-to-peak and CER values of pixels in the selected ROI's

6. CONCLUSION

6.1 General Conclusions

In this thesis, we designed and realized a program to quantitatively analyze Renal Perfusion MR images. We tested our program with MR images obtained from ten volunteers having normal renal functions. We computed signal intensity-time curves and functional parameters (Slope, Contrast Enhancement Ratio, Time-to-Peak). These parameters were also obtained for each pixel of the selected ROI's for comparison of the results.

A method is needed to compensate kidney motion due to the respiration. Two options are available: scanning with breath holding and the use of a movement correction algorithm. Scanning during breath holding (with intermittent breathing periods because a full scan takes at least two minutes) is potentially problematic for two main reasons. Firstly, the data series are interrupted at times when the patient is breathing and this may cause misinterpretation of the enhancement curve. Secondly, it has been shown that even during breath holding the kidney moves. Especially during breath holding after inhalation, which can be maintained longer than after exhalation, the diaphragm moves [11], so the kidney moves as well. This would render the entire exercise of breath holding useless.

We, therefore, chose to scan during free breathing, and then we corrected effects of the movement of the kidney in the images. With normal shallow breathing, the kidney only translates in the image. The rotation of the kidney is negligible and small shape changes occur due to minimal through plane movement. Since there is only translation of the kidneys, we can shift the entire image in the opposite direction to the movement. The other structures in the images are not used in the analysis so their misregistration is not important.

It was established that the additional noise was caused by unsaturated spins moving into the imaging slice. Using a multi-slice technique reduced the noise in the signal significantly and made the analysis more reliable.

A reliable manual segmentation of the kidney is only possible shortly after the arrival of the contrast agent to the kidney showing sufficient enhancement. Not the entire kidney border will show early enhancement; in the area of the renal pelvis there is no cortex and thus no enhancement. Since the outer layer of the kidney consists of cortex, it is easy to select a ROI to measure the cortical enhancement. However, it is usually impossible to find a ROI that gives a pure medullary signal without cortical contamination. The nephron path is highly organized, especially in the medulla. Therefore, the medulla is poorly discernable due to a complex course of the medulla-cortex tissue border, weak contrast and partial volume. Medullary enhancement is delayed with respect to cortical enhancement and this effect can be used to determine the cortical contribution to the enhancement signal in a ROI that contains cortical as well as medullary tissue.

In normal kidneys, the MRI SI-Time Curves exhibit the following typical phases after the contrast bolus delivery to the kidney by the circulation:

- The first segment shows a somewhat slower, almost linear increase to a peak maximum. This segment represents parenchymal transfer, and continues to increase as long as more of the contrast agent passes from the blood into the kidney tubules than is excreted into the collecting system. Only this segment is used to calculate function of the kidneys.
- The last segment reflects contrast elimination from the parenchyma into the collecting system.

6.2 Recommendations of Future Work

To date, renal functional MRI is used primarily in research. Its routine application is limited. This is partly due to the variety of recommended techniques most of which fail to offer a quantitative assessment of renal function comparable to that of scintigraphy. Furthermore, MRI is an expensive imaging modality when compared with excretory urography, ultrasound and scintigraphy. These difficulties will most likely will prevent renal functional MR from completely replacing radionuclide studies in the very near future. On the other hand, improvements in MR technology and better and easy-to-use and hopefully fully automatic postprocessing methods could make MRI ready for routine clinical evaluation in the future.

The following is a list of recommendations for future work:

1. The operator input for the movement correction can be reduced in order to improve the automation of the method and the performance of the movement correction algorithm can be increase with thicker slices.

2. It can be interesting to see 3D scan of the entire kidney. The implementation of a 3D scan to include the entire kidney can result in more reliable or useful data.

APPENDIX A. BASIC INTERFACE FOR RENAL PERFUSION ANALYSIS

A.1 Introduction

Our program is designed and developed in MATLAB environment as a toolbox. MATLAB has been chosen for our development environment because of its rich library for image and signal processing, its practical user interface toolkit and its common usage in this sort of studies at academic environment all over the world. The aim of this program is reading, displaying and analyzing renal perfusion MR images which are in DICOM format. The input of our images is in DICOM format because it allows us to use our application later for images coming from different vendors. In this chapter, the parts of this program are presented.

A.2 User Interface

To start the program, user should write “renalyse” and press “enter” at the Matlab command prompt. Then interface will be visible to user. The program is now ready for the analysis of the renal perfusion data sets.

The main window of the program that user interacts with is shown in Figure A.1. All the steps of the Renal Perfusion Analysis are integrated to this interface. The program includes different parts. Each part is for different steps of the Renal Perfusion Analysis.

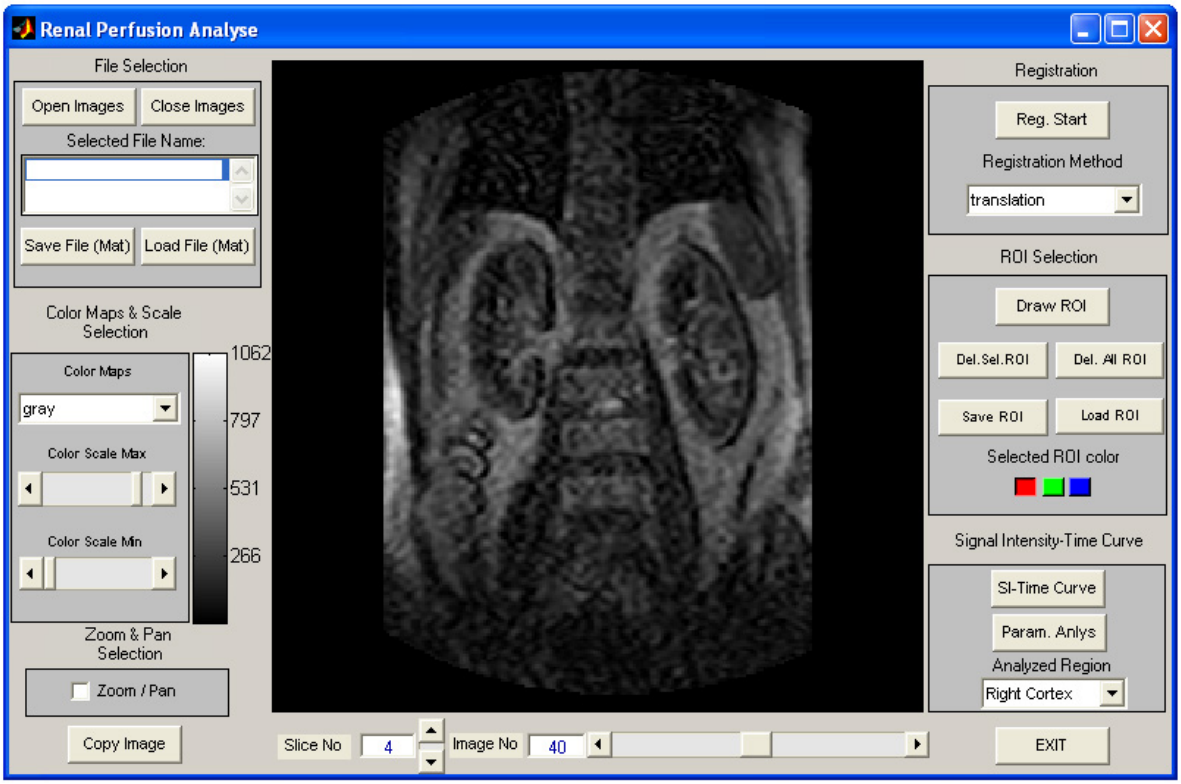

Figure A.1 User interface of Renalyse

A.3 File Selection

First part is "File Selection" area. In this area, users can open or can load image series and they can save or can close the existing image series. There is also a listbox in this area. The listbox shows the patient's name (Figure A.2).

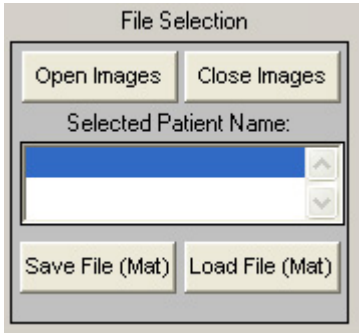

Figure A.2 File Selection

A.4 Image Display and Animation

The program displays and animates multi-slice renal datasets. The images can be resized, zoomed, and adjusted for brightness and contrast to provide a uniform display of all frames. The part of "Color Maps & Scale Selection" is for adjusting the display properties of the image (Figure A.3).

"Zoom & Pan Selection" area is used for zooming and panning. By checking the "Zoom/Pan" checkbox (Figure A.3), zooming and panning can be used with the left and right buttons of the mouse.

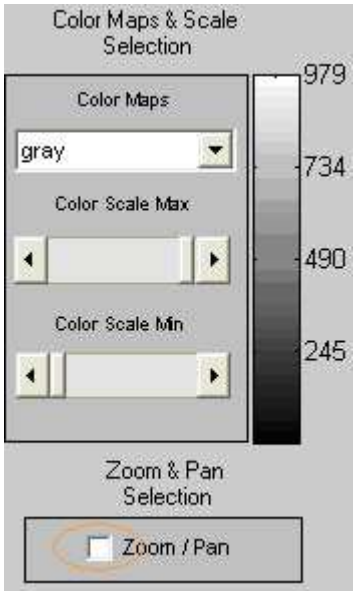

Figure A.3 Color Maps-Scale Selection and Zoom-Pan Selection

The other two sliders which is located under the image display area, are used for the selection of slice and image (Figure A.4).

Figure A.4 Slice and Image Selection

A.5 Registration

The image registration is performed on a region that the user interactively selected to encompass the kidney across the full range of respiratory motion. All shaped regions to be defined are supported (Figure A.5).

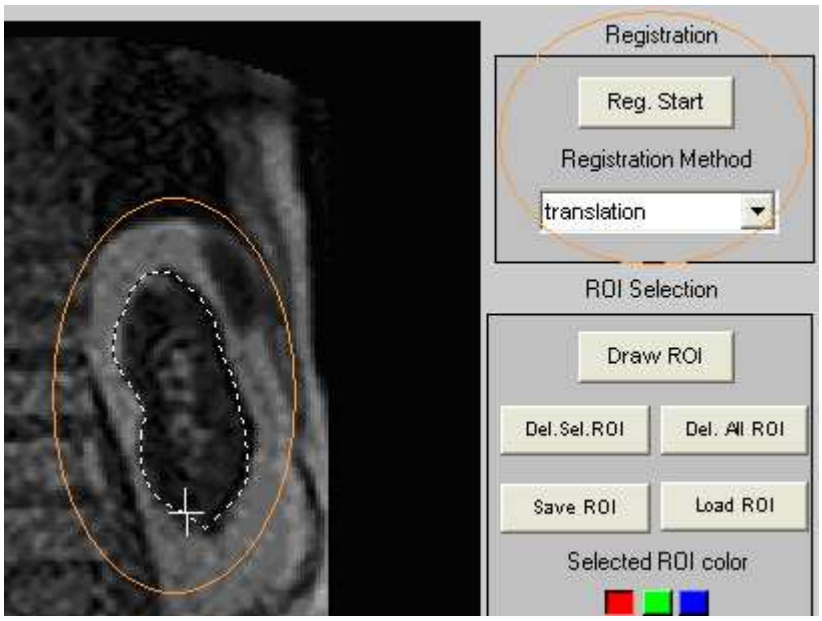

Figure A.5 Registration

"Registration" area located the right corner of the interface. First step is for registration process is to select the registration method. Then, by pushing the "Reg. Start" button, program will wait for the selection (left button of the mouse) of the registration region.

Selection will be completed with the right button of the mouse and registration will automatically start.

A.6 ROI Selection

After registration process is completed, the series with the registered images will display. The next step is ROI selection.

Users define the shape and location of the ROI within a registered image and the program automatically will copy this ROI on the other registered images. There are six buttons that can be used in the "ROI Selection" area. "Draw ROI" button is for selecting region of interest (users can select three different color for ROI lines) at the image (Figure A.6).

The other buttons are used for deleting the selected or all ROI's, saving the selected ROI and loading the saved ROI.

Figure A.6 ROI Selection

A.7 Signal Intensity-Time Curve

When the ROI Selection is finished, by pushing the "SI-Time Curve" button the Signal Intensity-Time curve for the selected ROI is plotted.

The "Analyzed Region" editbox is in the same area (Figure A.7). The selected analyzed region's name is showed in the title of the curve.

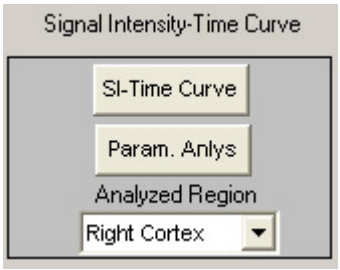

Figure A.7 Plotting the Signal Intensity-Time Curve

After pushing the “SI-Time Curve” and “Param. Anlys” buttons respectively, the mean signal intensity within the selected ROI for every image in the sequence is plotted against time, indexes of this curve are computed and parametric images of these indexes are displayed.

REFERENCES

1. Powers, T. A., C. H. Lorenz, G. E. Holburn, and R. Price, "Renal artery stenosis: in vivo perfusion MR imaging," *Radiology*, Vol. 178, pp. 543–548, 1991.

2. Hanna, S., O. Helenon, C. Legendre, J. F. Chiche, D. D. Stefano, H. Kreis, and J. F. Moreau, "MR imaging of renal transplant rejection," *Acta Radiology*, Vol. 32, pp. 42–46, January 1991.

3. Sharma, R., R. Gupta, and H. Poptani, "The magnetic resonance renogram in renal transplant evaluation using dynamic contrast enhanced MR imaging," *Transplantation*, no. 59, pp. 1405–1409, 1995.

4. Prasad, P. V., and A. Priatna, "Functional imaging of the kidneys with fast MRI techniques," *European Journal of Radiology*, Vol. 29, pp. 133–148, 1999.

5. Grenier, N., F. Basseau, M. Ries, B. Tyndal, R. Jones, and C. Moonen, "Functional MRI of the kidney," *Abdominal Imaging*, Vol. 28, pp. 164–175, 2003.

6. Roberts, T., "Physiology measurements by Contrast-Enhanced MR imaging: Expectations and limitations," *JMRI*, no. 7, pp. 82–90, 1997.

7. Fox, S. I., *Human Physiology*, Vol. 17, C.H. Whealty, 2002.

8. Cobelli, F., M. Venturini, A. Vanzulli, S. Sironi, M. Salvioni, E. Angeli, P. Scifo, M. P. Garancini, R. Quartagno, G. Bianchi, and A. Maschio, "Renal arterial stenosis: prospective comparison of color doppler US and breath-hold, three-dimensional, dynamic, gadolinium-enhanced MR angiography," *Radiology*, Vol. 214, pp. 373–380, 2000.

9. Hermoye, L., L. Annet, P. Lemmerling, F. Peeters, F. Jamar, P.Gianello, S. V. Huffel, and B. E. Beers, "Calculation of the renal perfusion and glomerular filtration rate from the renal impulse response obtained with MRI," *Magnetic Resonance in Medicine*, Vol. 51, pp. 1017–1025, 2004.

10. Choyke, P., J. Frank, and M. Girton, "Dynamic Gd-DTPA-enhanced MR imaging of the kidney: experimental results," *Radiology*, no. 170, pp. 713–720, 1989.

11. Bihan, D., E. Breton, D. Lallemand, P. Grenier, E. Cabanis, and J. M. Laval, "MR imaging of intravoxel incoherent motions: applications to diffusion and perfusion in neurologic disorder," *Radiology*, no. 161, p. 401407, 1986.

12. Bihan, D., "Molecular diffusion nuclear magnetic resonance imaging," *Magnetic Resonance Q*, Vol. 7, pp. 1–30, 1991.

13. Ros, P., J. Gauger, and C. Stoupis, "Diagnosis of renal artery stenosis: Feasibility of combining MR angiography, MR renography, and gadopentetate-based measurements of glomerular filtration rate," *AJR*, no. 165, pp. 1447–1451, 1995.

14. Krestin, G., G. Schuhmann-Giampieri, J. Haustein, G. Friedman, K. Neufang, W. Claub, and B. Stockl, "Functional dynamic MRI, pharmacokinetics and safety of Gd-DTPA in patients with impairedrenal function," *Eur J Radiology*, Vol. 2, p. 1623, 1992.

15. Takeda, M., Y. Katayama, T. Tsutui, T. Komeyama, and T. Mizusawa, "Does Gd-DTPA enhanced MRI of the kidney represent tissue concentration of contrast media in the kidney: in vivo and in vitro study?," *Magnatic Resonance Imaging*, Vol. 12, pp. 421–427, 1994.

16. Pauling, L., and C. D. Coryell, "The magnetic properties and structure of hemoglobin, oxyhemoglobin, and carbonmonoxyhemoglobin," *Proc Natl Acad Sci*, Vol. 22, no. 210-216, 1936.

17. Ogawa, S., T. M. L. A. R. Kay, and D. W. Tank, "Brain magnetic resonance imaging with contrast dependence on blood oxygenation," *Proc Natl Acad Sci*, Vol. 87, p. 98689872, 1990.

18. Grenier, N., H. Trillaud, and C. Combe, "Diagnosis of renovascular hypertension: Feasibility of captopril-sensitized dynamic MR imaging and comparison with captopril scintigraphy," *AJR*, no. 166, pp. 835–843, 1996.

19. Munechika, H., and D. Sullivan, "Evaluation of acute renal failure with magnetic resonance imaging using gradient-echo and Gd-DTPA," *Invest. Radiology*, no. 26, pp. 22–27, 1991.

20. Atle, B., "Proton properties of a particulate iron oxide MR contrast agent in different tissue systems implications for imaging." Comprehensive Summaries of Uppsala Dissertations from the Faculty of Medicine, 2002.

21. Kikinis, R., S. von G., and e. a. P. Jäger, "Normal and hydronephrotic kidney: Evaluation of renal function with contrast-enhanced MR imaging," *Radiology*, Vol. 165, pp. 837–842, 1987.

22. Ascher, S., J. Brown, and R. Colindres, "Renal corticomedullary differentiation: observation in patients with differing serum creatinine levels," *Radiology*, Vol. 190, pp. 149–152, 1994.

23. "The DICOM Standard." National Electrical Manufacturers Association, 2004. http://medical.nema.org/dicom/2004.html.

24. Semelka, R., H. Hricak, E. Tomei, A. Floth, and M. Stoller, "Obstructive nephropathy: Evaluation with dynamic Gd-DTPA-enhanced MR imaging," *Radiology*, no. 175, pp. 797–803, 1990.

25. Slavin, G. S., S. N. Gupta, P. L. Choyke, and T. K. F. Foo, "Rapid multi-slice renal perfusion MR imaging with simultaneous angiographic screening," in *Proc 10th Annual Meeting ISMRM*, (Honolulu), p. 2370, 2002.

26. Holland, A., J. Goldfarb, and R. Edelman, "Diaphragmatic and cardiac motion during suspended breathing: Preliminary experience and implications for breath-hold MR imaging," *Radiology*, Vol. 209, pp. 483–489, 1998.

27. Giele, E. L. W., J. Priester, J. A. Blom, J. A. Boer, J. M. A. Engelshoven, A. Hasman, and M. Geerlings, "Movement correction of the kidney in dynamic MRI scans using FFT phase difference movement detection," *Journal Of Magnetc Resonance Imagng*, Vol. 14, pp. 741–749, 2001.

28. Thevenaz, P., U. E. Ruttimann, and M. Unser, "Iterative multi-scale registration without landmarks," in *Proc.IEEE International Conference on Image Processing*, Vol. 3, (Washington DC USA), pp. 228–231, October 1995.

29. Thevenaz, P., U. E. Ruttimann, and M. Unser, "A pyramid approach to subpixel registration based on intensity," *IEEE Transactions on Image Processing*, Vol. 7, January 1998.

30. Gerig, G., R. Kikinis, W. Kuoni, G. K. Schulthess, and O. Kübler, "Semiautomated ROI analysis in dynamic MR studies. part I: image analysis tools for automatic correction of organ displacements," *JCAT*, no. 15, pp. 725–732, 1991.

31. Burger, P., J. Panting, P. Gatehouse, D. Rueckert, D. Penell, and D. Firmin, "Motion and deformation tracking for short-axis echo-planar myocardial perfusion imaging," *Medical Image Analysis*, no. 2, pp. 285–302, 1998.

32. Dietl, T. V. K., and A. Fahrenkamp, "Die Rindennekrose der Transplantatniere," *Röntgenstr*, Vol. 6, pp. 507–512, 1992.